Exact theory and approximations for optical resonators in a changing external medium

S. F. Almousa[1, 2] and E. A. Muljarov[1]

[1] *School of Physics and Astronomy, Cardiff University, Cardiff CF24 3AA, United Kingdom*
[2] *Department of Physics and Astronomy, King Saud University, Riyadh 11451, Saudi Arabia*

(Dated: January 23, 2023)

Finding reliably and efficiently the spectrum of the resonant states of an optical system under varying parameters of the medium surrounding it is a technologically important task, primarily due to various sensing applications. Computationally, it presents, however, a fundamental challenge owing to the nature of the eigenstates of an open system lacking completeness outside it. We solve this challenge by making a linear transformation of Maxwell's equations which maps perturbations of the surrounding medium onto effective perturbations within the system where the resonant states are complete. By treating such perturbations with the rigorous resonant-state expansion, we find the modified modes of the system for arbitrary homogeneous perturbations of the medium with any required accuracy. Numerically efficient single-mode approximation is shown to be highly accurate, as illustrated for various plasmonic nanoparticles, including gold nanospheres and silver bow-tie antennas.

Sensing the material surrounding an optical resonator by looking at its eigenmodes, such as localized surface plasmon (SP) modes in metallic nanoparticles [1] or whispering gallery (WG) modes in dielectric microspheres [2], has recently become an important application of nanophotonics. However, modelling and optimization of optical resonators for sensing applications, as well as interpreting the sensing information present complicated 'inverse' problems which require extensive and repetitive calculations. Theoretical approaches, in which the eigenmodes of the system are calculated only once and then used as a fixed basis for treating any changes of the environment, could reduce the computational time dramatically, by orders of magnitude, as has been recently demonstrated by a first-order perturbation theory [3]. At the same time, for a number of technologically crucial applications of optical resonators, such as the refractive index or chirality sensing, it is very important to develop a theory which would accurately and efficiently treat any changes of the medium and is not limited to first order. For example, the same optical resonator may be used as a sensor operating in different media surrounding it, which requires non-perturbative approaches.

Both in perturbative and non-perturbative approaches, treating external perturbations of an open optical system presents a fundamental challenge. The exponential growth with distance of the electromagnetic field of the eigenmodes of the system not only causes the well known issue with the mode normalization [4] but also results in a limited completeness of the eigenmodes outside the system. While the former has been recently solved by introducing an exact analytical normalization [5, 6] or by regularizing the exponentially growing fields [7, 8], the lack of completeness of regularized RSs in the exterior limits the accuracy of treating external perturbations to first order, as demonstrated in Sec. S.II of [9]. First- and second-order perturbation theories for open resonators treating finite-size volume perturbations [10–13] or boundary perturbations [14] or both together [15] are available in the literature. However, these approaches are not suitable for treating homogeneous perturbations of the entire space surrounding the system.

The resonant states (RSs) of an optical system, also known as quasi-normal modes [8], are the eigen solutions to Maxwell's equations with outgoing wave boundary conditions. They fully describe the spectral properties of an optical system, providing direct access to its scattering matrix [16, 17]. Their exact normalization consists of a sum of a volume integral of the square of the RS field with a material-dependent weight function, performed over any finite volume containing the system, and an integral of the fields over the volume surface [4–6]. Owing to the well-defined boundaries of an optical system, the RSs are complete at least within the minimal convex volume containing the system [6]. Such a completeness is at the heart of the resonant-state expansion (RSE), a rigorous method recently developed for treating perturbations of arbitrary shape and strength by mapping Maxwell's equations onto a linear matrix eigenvalue problem [5, 11]. The RSE has been generalized to include the frequency dispersion [18] as well as magnetic, chiral, and bi-anisotropic materials [6] and was proven to be orders of magnitude more efficient than popular computational methods [11, 19]. However, a significant limitation of the RSE is that all perturbations must be contained within the basis system.

Recently, a single-mode first-order perturbation theory capable of including homogeneous and isotropic perturbations of the surrounding medium has been developed [3]. This theory uses the analytic normalization of the RSs but treats perturbations in a way entirely different from the RSE. Crucially, it is limited to small perturbations and predicts only linear changes of the RS frequencies with the medium parameters, such as the permittivity. However, the optical modes can be extremely sensitive to even small changes of the environment. In

plasmonic resonators, for example, this can be due to strong near fields and hot spots. Also, single-mode theories fail when two or more RSs affected by perturbations are spectrally close to each other, such as in the examples considered in [20, 21]. At the same time, one and the same nanosensor may be operating in various solutions with a difference in the refractive index going significantly beyond first order.

In this Letter, we present a rigorous RSE-based approach to treating any changes of a homogeneous isotropic or bi-isotropic medium surrounding an optical system. By making a linear transformation of Maxwell's equations we map the changes of the surrounding medium onto effective perturbations of the system itself, which are then taken into account by the RSE. From this rigorous RSE-based approach we extract also a single-mode approximation and compare both with the first-order perturbation theory [3], which is presently the best available approximation.

Let us start assuming that the relevant RSs of a basis system are known. This basis system is an optical resonator described by generally dispersive permittivity and permeability tensors, respectively, $\hat{\boldsymbol{\varepsilon}}(k,\mathbf{r})$ and $\hat{\boldsymbol{\mu}}(k,\mathbf{r})$, where $k=\omega/c$ is the light wave number. The RSs are solutions to Maxwell's equations [6],

$$\left[k_n\hat{\mathbb{P}}_0(k_n,\mathbf{r})-\hat{\mathbb{D}}(\mathbf{r})\right]\vec{\mathbb{F}}_n(\mathbf{r})=0\,, \tag{1}$$

satisfying outgoing boundary conditions. Here,

$$\hat{\mathbb{P}}_0(k,\mathbf{r})=\begin{pmatrix}\hat{\boldsymbol{\varepsilon}}(k,\mathbf{r}) & \hat{\mathbf{0}}\\ \hat{\mathbf{0}} & \hat{\boldsymbol{\mu}}(k,\mathbf{r})\end{pmatrix},\quad \hat{\mathbb{D}}(\mathbf{r})=\begin{pmatrix}\hat{\mathbf{0}} & \nabla\times\\ \nabla\times & \hat{\mathbf{0}}\end{pmatrix}, \tag{2}$$

are, respectively, the 6×6 generalized permittivity and curl operators, $\vec{\mathbb{F}}_n(\mathbf{r})$ is a 6×1 column vector with components of the electric field $\mathbf{E}_n(\mathbf{r})$ and magnetic field $i\mathbf{H}_n(\mathbf{r})$, $\hat{\mathbf{0}}$ is the 3×3 zero matrix, and n is an index labelling the RSs. Let us use $\mathcal{V}_{\rm in}$ and $\mathcal{V}_{\rm out}$ to denote, respectively, the system volume and the rest of space. Let us also assume that the basis system is surrounded by an isotropic homogeneous medium described by $\hat{\mathbb{P}}_0(k,\mathbf{r})=\left[\varepsilon_{b_0}(k)\hat{\mathbf{1}};\mu_{b_0}(k)\hat{\mathbf{1}}\right]$ for $\mathbf{r}\in\mathcal{V}_{\rm out}$, where $\varepsilon_{b_0}(k)$ and $\mu_{b_0}(k)$ are, respectively, the medium permittivity and permeability, $\hat{\mathbf{1}}$ is the 3×3 identity matrix, and the brackets are used for writing block-diagonal tensors, such as $\hat{\mathbb{P}}_0(k,\mathbf{r})$ in Eq. (2).

Now, we consider a perturbed system which is the same optical resonator but placed in a different environment, so its RSs (labelled with index ν) are modified and satisfy perturbed Maxwell's equations

$$\left[k_\nu\hat{\mathbb{P}}(k_\nu,\mathbf{r})-\hat{\mathbb{D}}(\mathbf{r})\right]\vec{\mathbb{F}}_\nu(\mathbf{r})=0 \tag{3}$$

with $\hat{\mathbb{P}}(k,\mathbf{r})=\hat{\mathbb{P}}_0(k,\mathbf{r})=[\hat{\boldsymbol{\varepsilon}}(k,\mathbf{r});\hat{\boldsymbol{\mu}}(k,\mathbf{r})]$ for $\mathbf{r}\in\mathcal{V}_{\rm in}$ and $\hat{\mathbb{P}}(k,\mathbf{r})=\left[\varepsilon_b(k)\hat{\mathbf{1}};\mu_b(k)\hat{\mathbf{1}}\right]$ for $\mathbf{r}\in\mathcal{V}_{\rm out}$. A more general case of bi-isotropic systems is treated in Sec. S.I of [9]. Also, in what follows, we assume that both the unperturbed and perturbed permittivity and permeability of the surrounding medium are frequency independent; the case of dispersive medium is considered in Sec. S.II of [9] by using the RS regularization.

Introducing re-scaled fields $\mathbf{E}$ and $\mathbf{H}$ and wave number k, defined by

$$\mathbf{E}_\nu(\mathbf{r})=\alpha\mathbf{E}\,,\qquad \mathbf{H}_\nu(\mathbf{r})=\beta\mathbf{H}\,,\qquad k_\nu=\Gamma k\,, \tag{4}$$

where $\alpha=\sqrt{\frac{\varepsilon_{b_0}}{\varepsilon_b}}$, $\beta=\sqrt{\frac{\mu_{b_0}}{\mu_b}}$, and $\Gamma=\alpha\beta$, Eq. (3) becomes

$$\left[k\hat{\mathbb{P}}_0(k,\mathbf{r})+k\Delta\hat{\mathbb{P}}(k,\mathbf{r})-\hat{\mathbb{D}}(\mathbf{r})\right]\vec{\mathbb{F}}(\mathbf{r})=0\,. \tag{5}$$

where the perturbation $\Delta\hat{\mathbb{P}}(k,\mathbf{r})=0$ for $\mathbf{r}\in\mathcal{V}_{\rm out}$ and $\Delta\hat{\mathbb{P}}(k,\mathbf{r})=[\Delta\hat{\boldsymbol{\varepsilon}}(k,\mathbf{r});\Delta\hat{\boldsymbol{\mu}}(k,\mathbf{r})]$ for $\mathbf{r}\in\mathcal{V}_{\rm in}$, with

$$\Delta\hat{\boldsymbol{\varepsilon}}(k,\mathbf{r}) = \alpha^2\hat{\boldsymbol{\varepsilon}}(\Gamma k,\mathbf{r})-\hat{\boldsymbol{\varepsilon}}(k,\mathbf{r}) \tag{6}$$

$$\Delta\hat{\boldsymbol{\mu}}(k,\mathbf{r}) = \beta^2\hat{\boldsymbol{\mu}}(\Gamma k,\mathbf{r})-\hat{\boldsymbol{\mu}}(k,\mathbf{r})\,. \tag{7}$$

The transformed Eq. (5) describes an effective perturbed system which is surrounded by the same medium as the unperturbed one, with the perturbation moved from the outside to the inside. As the effective perturbation is concentrated within the system volume only, one can solve Eq. (5) via the dispersive RSE, with the unperturbed system described by Eq. (1) and the basis RSs given by k_n and $\vec{\mathbb{F}}_n(\mathbf{r})$.

We solve Eq. (5) by expanding the perturbed RS into the unperturbed ones,

$$\vec{\mathbb{F}}(\mathbf{r})=\sum_n c_n\vec{\mathbb{F}}_n(\mathbf{r})\,.$$

Then, according to the dispersive RSE [6, 18], the perturbed RS wave number k of the effective system and the expansion coefficients c_n satisfy a matrix eigenvalue equation

$$\begin{aligned}(k-k_n)c_n &= -k\sum_m V_{nm}(\infty)c_m\\ &\quad +k_n\sum_m\left[V_{nm}(\infty)-V_{nm}(k_n)\right]c_m\,,\end{aligned} \tag{8}$$

which is linear in k, and where

$$V_{nm}(k)=\int\vec{\mathbb{F}}_n(\mathbf{r})\cdot\Delta\hat{\mathbb{P}}(k,\mathbf{r})\vec{\mathbb{F}}_m(\mathbf{r})d\mathbf{r}\,. \tag{9}$$

Equation (8) is an exact result provided that all the RSs are included in the basis. It is valid for an arbitrary generalized Drude-Lorentz dispersion of the generalized permittivity,

$$\hat{\mathbb{P}}_0(k,\mathbf{r})=\hat{\mathbb{P}}_\infty(\mathbf{r})+\sum_j\frac{\hat{\mathbb{Q}}_j(\mathbf{r})}{k-\Omega_j}\,, \tag{10}$$

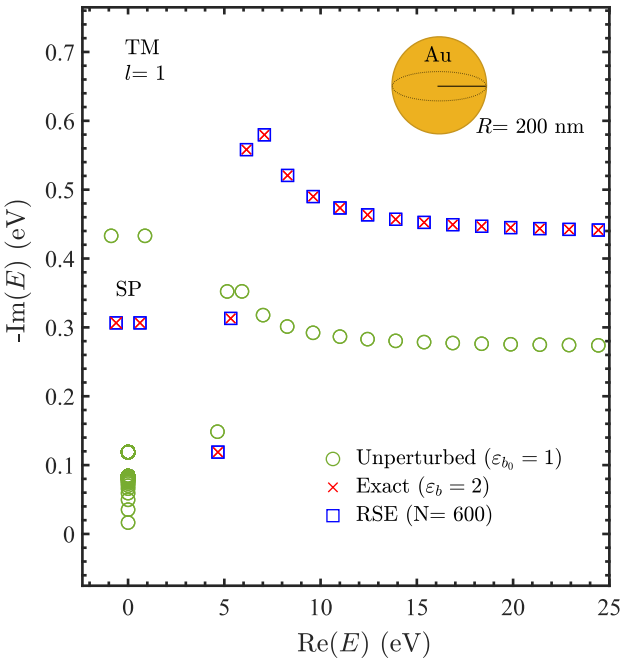

FIG. 1. Complex energies $E = \hbar ck$ of the RSs of a gold nanosphere of radius $R = 200\,\text{nm}$, surrounded by vacuum (open circles) and by a dielectric with $\varepsilon_b = 2$, calculated by the RSE (squares) and analytically (×), for TM polarization and $l = 1$.

where the generalized conductivity $\hat{\mathbb{Q}}_j(\mathbf{r})$ is the residue of $\hat{\mathbb{P}}_0(k,\mathbf{r})$ at the pole $k = \Omega_j$ in the complex frequency plane [22]. Note that the poles of $\hat{\mathbb{P}}_0(k,\mathbf{r}) + \Delta\hat{\mathbb{P}}(k,\mathbf{r})$ and $\hat{\mathbb{P}}_0(k,\mathbf{r})$ are generally different for $\Gamma \neq 1$, so that $\Delta\hat{\mathbb{P}}(k,\mathbf{r})$ replaces one group of poles with another. Both groups are to be taken into account in the basis and treated by the infinitesimal-dispersive RSE (idRSE) [23].

Keeping only diagonal terms in Eq. (8) results in a single-mode approximation,

$$k_\nu = \Gamma k \approx \Gamma k_n \frac{1 + V_{nn}(\infty) - V_{nn}(k_n)}{1 + V_{nn}(\infty)}\,, \qquad (11)$$

which turns out to be surprisingly accurate for a large class of plasmonic nano-resonators, as we demonstrate below and in Sec. S.V of [9].

The first-order contribution of the surrounding medium to the RS wave number [3] can be extracted directly from Eq. (11), assuming that the relative changes of the permittivity and permeabilities are small, i.e. $|\delta_\varepsilon|$, $|\delta_\mu| \ll 1$, where $\delta_\varepsilon = \varepsilon_b/\varepsilon_{b_0} - 1$ and $\delta_\mu = \mu_b/\mu_{b_0} - 1$. This gives (for derivation, see Sec. S.I of [9])

$$k_\nu \approx k_n + \frac{1}{2}(q_n^E - k_n)\delta_\varepsilon + \frac{1}{2}(q_n^H - k_n)\delta_\mu\,, \qquad (12)$$

where

$$q_n^E = \int_{\mathcal{V}_{\text{in}}} \left[\mathbf{E}_n \cdot (k^2\hat{\boldsymbol{\varepsilon}})'\mathbf{E}_n - k_n^2 \mathbf{H}_n \cdot \hat{\boldsymbol{\mu}}'\mathbf{H}_n\right] d\mathbf{r}\,, \qquad (13)$$

$$q_n^H = \int_{\mathcal{V}_{\text{in}}} \left[k_n^2 \mathbf{E}_n \cdot \hat{\boldsymbol{\varepsilon}}'\mathbf{E}_n - \mathbf{H}_n \cdot (k^2\hat{\boldsymbol{\mu}})'\mathbf{H}_n\right] d\mathbf{r}\,, \qquad (14)$$

and the primes denote the derivatives with respect to the wave number k, all taken at $k = k_n$. For a non-dispersive surrounding medium, this result is identical to the first-order approximation presented in [3]; its analogue for a dispersive medium considered in Sec. S.II of [9] is also shown to be identical to [3] in first order.

We illustrate in Figs. 1–4 the full RSE Eq. (8), its diagonal version Eq. (11), and the first-order approximation Eq. (12). Figure 1 shows in the complex energy plane ($E = \hbar ck$) the spectrum of the transverse-magnetic (TM) RSs with orbital momentum $l = 1$ of a gold nanosphere of radius $R = 200\,\text{nm}$ surrounded by a dielectric with $\varepsilon_b = 2$, calculated analytically and via the RSE, using as basis system the same sphere in vacuum. The dipolar SP mode is further investigated in Figs. 2 and 3, varying, respectively, the background permittivity ε_b and the sphere radius R, the latter taking values between 10 nm and 200 nm – a similar size range of plasmonic nanoparticles is used in experiments [24]. The permittivity is

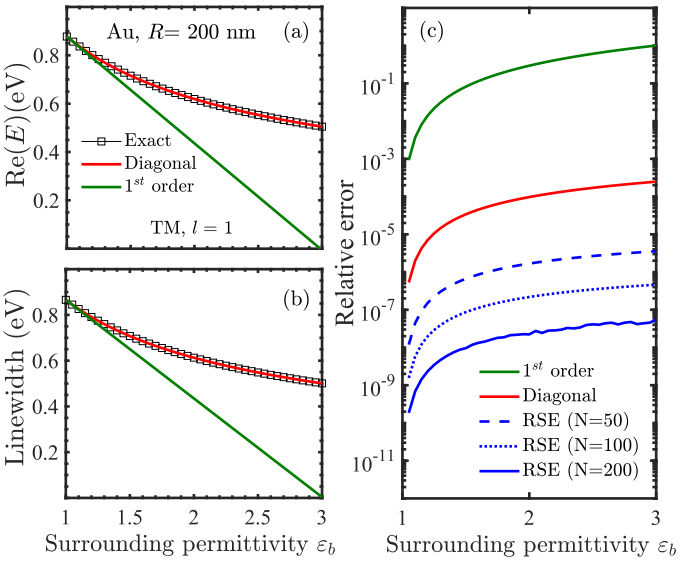

FIG. 2. (a) Resonance energy (Re E), (b) linewidth (-Im E), and (c) relative error of the complex energy E of the fundamental SP mode of a gold nanosphere ($R = 200\,\text{nm}$) as functions of the background permittivity ε_b, calculated analytically (thin black lines with open squares), using the diagonal dispersive RSE (red lines) and first-order approximation (green lines). (c) Relative error of the first-order (green) and diagonal approximation (solid red line), as well as of the full RSE with $N = 50$ (dashed blue), 100 (dotted blue) and 200 (solid blue line).

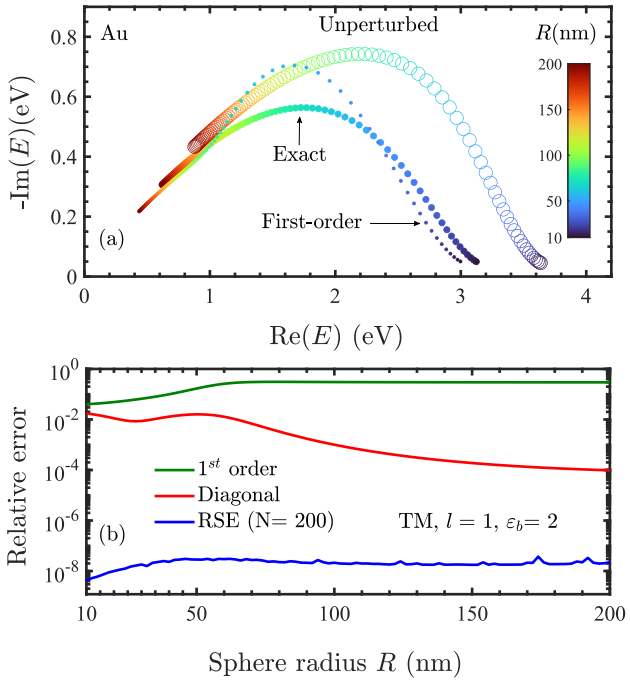

FIG. 3. (a) Complex energy of the fundamental SP mode of a gold nanosphere surrounded by vacuum (unperturbed) and by a dielectric with $\varepsilon_b = 2$ (exact and first-order) as functions of the sphere radius R given by the color code. (b) Relative error of first-order (green) and diagonal approximation (red), as well as of the full RSE (blue line), as functions of R.

taken in the Drude model, $\varepsilon(k) = \varepsilon_\infty - \sigma\gamma/[k(k+i\gamma)]$, with $\varepsilon_\infty = 4$, $\hbar c\sigma = 957\,\text{eV}$, and $\hbar c\gamma = 0.084\,\text{eV}$, fitted to the Johnson and Christy data [25] with the help of the fit program provided in [22]. In the full RSE calculation via Eq. (8), the only numerical parameter is the number N of the basis RSs which is determined by the cut-off frequency k_c, such that all RSs with k_n within the circle $|k_n\sqrt{\varepsilon(k_n)}| < k_c$ in the complex wave number plane are kept in the basis.

Since the perturbation shifts the unperturbed Drude pole of the permittivity at $k = -i\gamma$ to a new position at $k = -i\gamma/\Gamma$, we apply the idRSE which requires including in the basis both the old and the new pole RSs (pRSs) [23]. This is crucial for the RSE convergence to the exact solution, as it is clear from Fig. S4 of [9]. In fact, with pRSs included in the basis, the relative error shown in Fig. 2(c) scales with the basis size as $1/N^3$, as expected from the RSE [5, 11]. At the same time, the pRSs of the new pole in the idRSE are perturbation-dependent which makes the whole calculation rather inefficient. To avoid this problem, we have replaced the new pRSs with the old ones adapted for the perturbation, as detailed in Sec. S.IV of [9], so that all the basis RSs are calculated only once for all perturbations of the environment.

Figures 2 and 3 show also the diagonal approximation for the SP mode which turns out to be extremely accurate for any size of a plasmonic resonator, as it is clear from Fig. 3(b). The first-order approximation instead fails when ε_b has moderate or even small deviation from ε_{b_0}, as it is clear from Fig. 2. Sections S.II and S.V of [9] provide also a comparison with other approximations, including a RS regularization.

Focusing on single-mode and first-order approximations, Eqs. (11) and (12), respectively, we further demonstrate that the quality of these approximations is almost independent of the shape and even the material of the resonator. To evaluate the diagonal matrix elements of the perturbation in Eqs. (11) and (12) for the RSs calculated numerically, we exploit the accuracy of the diagonal approximation Eq. (11) and introduce in Sec. S.V.D of [9] a practical method to calculate the integrals by using only the wave numbers of the unperturbed and slightly perturbed RSs, without using any explicit RS normalization.

An example provided in Fig. 4 is a silver bow-tie antenna having dimensions shown in the inset. The Drude parameters of silver are again generated by [22], giving $\varepsilon_\infty = 1$, $\hbar c\sigma = 4157\,\text{eV}$, and $\hbar c\gamma = 0.018\,\text{eV}$. The fundamental SP mode of the bow-tie antenna in vacuum, having the electric field shown in Fig. 4(c), is used as basis state for the single-mode and first-order approxima-

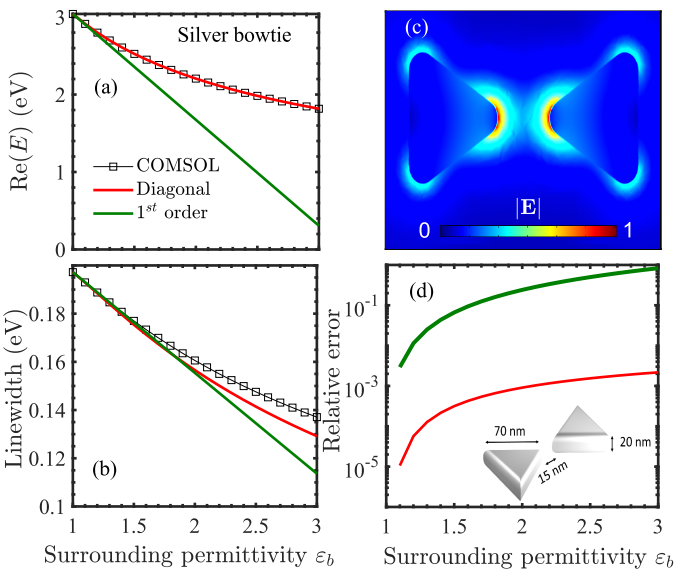

FIG. 4. (a) Resonance energy and (b) linewidth of the fundamental SP mode of a silver bow-tie antenna as functions of the permittivity of the surrounding medium ε_b, calculated using COMSOL [26] (black squares), diagonal and the first-order approximations (red and green lines, respectively). (c) Electric field of the unperturbed SP mode. (d) Error of the diagonal (red line) and first-order approximation (green line) relative to COMSOL data. The inset shows schematics and dimensions of the system, with corners rounded to arcs with a radius of 8 nm.

tions. The mode is calculated with a COMSOL extension MAN-7.1 [26, 27], and for other values of ε_b is used for visual comparison in Fig. 4(a,b) and error evaluation in Fig. 4(d). The relative errors are quantitatively similar to those obtained for a silver sphere of radius $R = 40\,\mathrm{nm}$ presented in Fig. S14(d) of [9] and are qualitatively similar to those of a gold sphere in Figs. 2(c) and 3(b). We see, in particular that the diagonal approximation works the same way for nanoparticles of different shapes and materials. For more details and other examples, such as a silver dolmen and silica micro-sphere resonators, and for comparison with other approximations, see Sec. S.V of [9].

In conclusion, we have developed a rigorous and efficient RSE-based approach to treating arbitrarily strong homogeneous perturbations of the medium surrounding an optical system, which is crucial for sensing applications. The idea of the approach is to map the changes in the surrounding medium onto the interior of the system, where the resonant states are complete, in this way effectively modifying the resonator while keeping the medium unchanged. Such a modified system is then treated by the RSE which requires a basis of resonant states fixed for all perturbations, with the basis size N determining the accuracy and the error scaling as $1/N^3$. The developed single-mode approximation is shown to be very accurate for plasmonic nanoparticles, going significantly beyond the first-order theory [3].

Acknowledgements: The authors thank W. Langbein for discussions. S. F. A. acknowledges support by King Saud University.

[1] A. Unger and M. Kreiter, Analyzing the performance of plasmonic resonators for dielectric sensing, The Journal of Physical Chemistry C **113**, 12243 (2009).

[2] S. Arnold, M. Khoshsima, I. Teraoka, S. Holler, and F. Vollmer, Shift of whispering-gallery modes in microspheres by protein adsorption, Opt. Lett. **28**, 272 (2003).

[3] S. Both and T. Weiss, First-order perturbation theory for changes in the surrounding of open optical resonators, Opt. Lett. **44**, 5917 (2019).

[4] E. A. Muljarov and W. Langbein, Exact mode volume and purcell factor of open optical systems, Phys. Rev. B **94**, 235438 (2016).

[5] E. A. Muljarov, W. Langbein, and R. Zimmermann, Brillouin-wigner perturbation theory in open electromagnetic systems, Europhys Lett. **92**, 50010 (2010).

[6] E. A. Muljarov and T. Weiss, Resonant-state expansion for open optical systems: generalization to magnetic, chiral, and bi-anisotropic materials, Opt. Lett. **43**, 1978 (2018).

[7] A. Baz', Y. Zel'dovich, and A. Perelomov, *Scattering, Reactions and Decay in Nonrelativistic Quantum Mechanics* (U. S. Department of Commerce, Washington, D. C., 1969).

[8] C. Sauvan, J. P. Hugonin, I. S. Maksymov, and P. Lalanne, Theory of the spontaneous optical emission of nanosize photonic and plasmon resonators, Phys. Rev. Lett. **110**, 237401 (2013).

[9] S. F. Almousa and E. A. Muljarov, *Supplementary Information* (2021).

[10] P. T. Leung and K. M. Pang, Completeness and time-independent perturbation of morphology-dependent resonances in dielectric spheres, JOSA B **13**, 805–817 (1996).

[11] M. B. Doost, W. Langbein, and E. A. Muljarov, Resonant-state expansion applied to three-dimensional open optical systems, Phys. Rev. A **90**, 013834 (2014).

[12] J. Yang, H. Giessen, and P. Lalanne, Simple analytical expression for the peak-frequency shifts of plasmonic resonances for sensing, Nano Letters **15**, 3439–3444 (2015).

[13] A. Gras, W. Yan, and P. Lalanne, Quasinormal-mode analysis of grating spectra at fixed incidence angles, Opt. Lett. **44**, 3494 (2019).

[14] W. Yan, P. Lalanne, and M. Qiu, Shape deformation of nanoresonator: A quasinormal-mode perturbation theory, Phys. Rev. Lett. **125**, 013901 (2020).

[15] Z. Sztranyovszky, W. Langbein, and E. A. Muljarov, First-order perturbation theory of eigenmodes for systems with interfaces, arXiv:2205.13041 (2022).

[16] S. V. Lobanov, W. Langbein, and E. A. Muljarov, Resonant-state expansion of three-dimensional open optical systems: Light scattering, Phys. Rev. A **98**, 033820 (2018).

[17] T. Weiss and E. A. Muljarov, How to calculate the pole expansion of the optical scattering matrix from the resonant states, Phys. Rev. B **98**, 085433 (2018).

[18] E. A. Muljarov and W. Langbein, Resonant-state expansion of dispersive open optical systems: Creating gold from sand, Phys. Rev. B **93**, 075417 (2016).

[19] S. V. Lobanov, G. Zoriniants, W. Langbein, and E. A. Muljarov, Resonant-state expansion of light propagation in nonuniform waveguides, Phys. Rev. A **95**, 053848 (2017).

[20] T. Weiss, M. Schäferling, H. Giessen, N. A. Gippius, S. G. Tikhodeev, W. Langbein, and E. A. Muljarov, Analytical normalization of resonant states in photonic crystal slabs and periodic arrays of nanoantennas at oblique incidence, Phys. Rev. B **96**, 045129 (2017).

[21] M. Mesch, T. Weiss, M. Schäferling, M. Hentschel, R. S. Hegde, and H. Giessen, Highly sensitive refractive index sensors with plasmonic nanoantennas – utilization of optimal spectral detuning of fano resonances, ACS Sensors **3**, 960 (2018).

[22] H. S. Sehmi, W. Langbein, and E. A. Muljarov, Optimizing the drude-lorentz model for material permittivity: Method, program, and examples for gold, silver, and copper, Phys. Rev. B **95**, 115444 (2017).

[23] H. S. Sehmi, W. Langbein, and E. A. Muljarov, Applying the resonant-state expansion to realistic materials with frequency dispersion, Phys. Rev. B **101**, 045304 (2020).

[24] L. M. Payne, W. Albrecht, W. Langbein, and P. Borri, The optical nanosizer – quantitative size and shape analysis of individual nanoparticles by high-throughput wide-field extinction microscopy, Nanoscale **12**, 16215 (2020).

[25] P. B. Johnson and R. W. Christy, Optical constants of the noble metals, Phys. Rev. B **6**, 4370 (1972).

[26] Modal Analysis of Nanoresonators (MAN-7.1) (https://www.lp2n.institutoptique.fr/light-complex-nanostructures).

[27] W. Yan, R. Faggiani, and P. Lalanne, Rigorous modal analysis of plasmonic nanoresonators, Phys. Rev. B **97**, 205422 (2018).

Supplementary information to "Exact theory and approximations for optical resonators in a changing external medium"

S. F. Almousa[1,2] and E. A. Muljarov[1]

[1]*School of Physics and Astronomy, Cardiff University, Cardiff CF24 3AA, United Kingdom*

[2]*Department of Physics and Astronomy, King Saud University, Riyadh 11451, Saudi Arabia*

(Dated: January 23, 2023)

S.I. GENERALIZATION OF THE RSE FOR PERTURBATIONS OF THE SURROUNDING MEDIUM

In this section, we generalize the resonant-state expansion (RSE) for perturbations of the surrounding medium which is assumed to be homogeneous and generally bi-isotropic (reduced to isotropic for zero Tellegan and Pasteur parameters), both with and without perturbation. We also assume throughout this work that both the system and the surrounding medium are reciprocal. The perturbed background medium is described by isotropic constants ε_b, μ_b, ξ_b, and ζ_b, providing linear relations between the electric and magnetic fields,

$$\mathbf{D} = \varepsilon_b \mathbf{E} + \xi_b \mathbf{H}\,, \qquad \mathbf{B} = \mu_b \mathbf{H} + \zeta_b \mathbf{E}\,. \tag{S1}$$

The constants ξ_b and ζ_b can be written as

$$\xi_b = \chi_b - i\varkappa_B = i\eta_b\,, \qquad \zeta_b = \chi_b + i\varkappa_b = -i\eta_b^*\,, \tag{S2}$$

and can both be expressed in terms of a single complex parameter

$$\eta_b = -\varkappa_b - i\chi_b\,, \tag{S3}$$

where χ_b and $\varkappa_b$ are, respectively, the Tellegen and Pasteur parameters of the medium.

Maxwell's equations in such a homogeneous medium take the form [S1]

$$k\hat{\mathbb{P}}_b\vec{\mathbb{F}} - \hat{\mathbb{D}}\vec{\mathbb{F}} = 0\,, \tag{S4}$$

where $k = \omega/c$ is the light wave number, and

$$\hat{\mathbb{P}}_b = \begin{pmatrix} \varepsilon_b\hat{\mathbf{1}} & \eta_b\hat{\mathbf{1}} \\ \eta_b^*\hat{\mathbf{1}} & \mu_b\hat{\mathbf{1}} \end{pmatrix}, \qquad \hat{\mathbb{D}} = \begin{pmatrix} \hat{\mathbf{0}} & \nabla\times \\ \nabla\times & \hat{\mathbf{0}} \end{pmatrix}, \qquad \vec{\mathbb{F}} = \begin{pmatrix} \mathbf{E} \\ i\mathbf{H} \end{pmatrix}, \tag{S5}$$

with $\hat{\mathbf{1}}$ and $\hat{\mathbf{0}}$ being, respectively, 3×3 identity and zero matrices.

Let us introduce a linear transformation which keeps the operator $\hat{\mathbb{D}}$ in Eq. (S4) unchanged. It is defined by

$$T\begin{pmatrix} 0 & 1 \\ 1 & 0 \end{pmatrix} S = \begin{pmatrix} 0 & 1 \\ 1 & 0 \end{pmatrix}, \tag{S6}$$

where T and S are 2×2 matrices having a general form

$$T = \frac{1}{\sqrt{\Delta}}\begin{pmatrix} \alpha & i\gamma \\ -i\delta & \beta \end{pmatrix}, \qquad S = \frac{1}{\sqrt{\Delta}}\begin{pmatrix} \alpha & i\delta \\ -i\gamma & \beta \end{pmatrix}, \tag{S7}$$

with

$$\Delta = \alpha\beta - \gamma\delta \tag{S8}$$

and α, β, γ, and δ arbitrary complex numbers. However, since the generalized permittivity matrix $\hat{\mathbb{P}}_b$ must be Hermitian, both with and without perturbation, they all have to be taken real. In fact, a reduced 2×2 Hermitian matrix of generalized permittivity,

$$P_b = \begin{pmatrix} \varepsilon_b & \eta_b \\ \eta_b^* & \mu_b \end{pmatrix},$$

is transformed according to

$$\begin{aligned} P_b' = TP_bS &= \frac{1}{\Delta}\begin{pmatrix} \alpha & i\gamma \\ -i\delta & \beta \end{pmatrix}\begin{pmatrix} \varepsilon_b & \eta_b \\ \eta_b^* & \mu_b \end{pmatrix}\begin{pmatrix} \alpha & i\delta \\ -i\gamma & \beta \end{pmatrix} \\ &= \frac{1}{\Delta}\begin{pmatrix} \alpha^2\varepsilon_b + \gamma^2\mu_b - \alpha\gamma i(\eta_b - \eta_b^*) & i(\alpha\delta\varepsilon_b + \gamma\beta\mu_b) + \alpha\beta\eta_b - \gamma\delta\eta_b^* \\ -i(\alpha\delta\varepsilon_b + \gamma\beta\mu_b) + \alpha\beta\eta_b^* - \gamma\delta\eta_b & \delta^2\varepsilon_b + \beta^2\mu_b - \delta\beta i(\eta_b - \eta_b^*) \end{pmatrix} \end{aligned} \tag{S9}$$

from what follows that α, β, γ, and δ are real, and $T = S^\dagger$. To complete the transformation of Eq. (S4), we also introduce wave number scaling,

$$k = \Gamma\tilde{k}\,, \tag{S10}$$

and require that

$$\tilde{P}_b = \Gamma P_b' = P_{b_0} \equiv \begin{pmatrix} \varepsilon_{b_0} & \eta_{b_0} \\ \eta_{b_0}^* & \mu_{b_0} \end{pmatrix}, \tag{S11}$$

where $\varepsilon_{b_0}, \mu_{b_0}$, and $\eta_{b_0} = -\varkappa_{b_0} - i\chi_{b_0}$ are the parameters of the unperturbed medium. This results in the following four equations determining Γ, α, β, γ, and δ:

$$\begin{aligned} \varepsilon_{b_0} &= \frac{\Gamma}{\Delta}\left(\alpha^2\varepsilon_b + \gamma^2\mu_b - 2\alpha\gamma\chi_b\right), \qquad \chi_{b_0} = -\frac{\Gamma}{\Delta}\left(\alpha\delta\varepsilon_b + \gamma\beta\mu_b - (\alpha\beta+\gamma\delta)\chi_b\right), \\ \mu_{b_0} &= \frac{\Gamma}{\Delta}\left(\delta^2\varepsilon_b + \beta^2\mu_b - 2\delta\beta\chi_b\right), \qquad \varkappa_{b_0} = \Gamma\varkappa_b\,. \end{aligned} \tag{S12}$$

Note that α, β, γ, and δ are defined up to an arbitrary constant factor, so that the number of the above equations is equal to the number of unknowns.

After applying the above transformation, the perturbed Maxwell equations in the surrounding medium take exactly the same form as the unperturbed ones,

$$\tilde{k}\begin{pmatrix} \varepsilon_{b_0}\hat{\mathbf{1}} & \eta_{b_0}\hat{\mathbf{1}} \\ \eta_{b_0}^*\hat{\mathbf{1}} & \mu_{b_0}\hat{\mathbf{1}} \end{pmatrix}\begin{pmatrix} \tilde{\mathbf{E}} \\ i\tilde{\mathbf{H}} \end{pmatrix} - \begin{pmatrix} \hat{\mathbf{0}} & \nabla\times \\ \nabla\times & \hat{\mathbf{0}} \end{pmatrix}\begin{pmatrix} \tilde{\mathbf{E}} \\ i\tilde{\mathbf{H}} \end{pmatrix} = 0\,, \tag{S13}$$

provided that the electromagnetic fields are also transformed according to

$$\begin{pmatrix} \mathbf{E} \\ i\mathbf{H} \end{pmatrix} = \frac{1}{\sqrt{\Delta}}\begin{pmatrix} \alpha & i\delta \\ -i\gamma & \beta \end{pmatrix}\begin{pmatrix} \tilde{\mathbf{E}} \\ i\tilde{\mathbf{H}} \end{pmatrix} = \frac{1}{\sqrt{\Delta}}\begin{pmatrix} \alpha\tilde{\mathbf{E}} - \delta\tilde{\mathbf{H}} \\ -i\gamma\tilde{\mathbf{E}} + i\beta\tilde{\mathbf{H}} \end{pmatrix}. \tag{S14}$$

Note that Eq. (S14) determines the field transformation in the entire space. Therefore, within the system, the transformed Maxwell's equations for a perturbed RS with the wave number $k_\nu = \Gamma\tilde{k}$ and the field $\vec{\mathbb{F}}_\nu = \hat{\mathbb{S}}\vec{\tilde{\mathbb{F}}}$ become

$$\tilde{k}\hat{\tilde{\mathbb{P}}}(\Gamma\tilde{k}, \mathbf{r})\vec{\tilde{\mathbb{F}}}(\mathbf{r}) - \hat{\mathbb{D}}(\mathbf{r})\vec{\tilde{\mathbb{F}}}(\mathbf{r}) = 0\,, \tag{S15}$$

where the generalized permittivity tensor,

$$\tilde{\hat{\mathbb{P}}}(k,\mathbf{r}) = \Gamma\hat{\mathbb{S}}^{\dagger}\hat{\mathbb{P}}_0(k,\mathbf{r})\hat{\mathbb{S}} = \frac{\Gamma}{\Delta}\begin{pmatrix} \alpha\hat{\mathbf{1}} & i\gamma\hat{\mathbf{1}} \\ -i\delta\hat{\mathbf{1}} & \beta\hat{\mathbf{1}} \end{pmatrix}\begin{pmatrix} \hat{\boldsymbol{\varepsilon}}(k,\mathbf{r}) & \hat{\boldsymbol{\eta}}(k,\mathbf{r}) \\ \hat{\boldsymbol{\eta}}^{*}(k,\mathbf{r}) & \hat{\boldsymbol{\mu}}(k,\mathbf{r}) \end{pmatrix}\begin{pmatrix} \alpha\hat{\mathbf{1}} & i\delta\hat{\mathbf{1}} \\ -i\gamma\hat{\mathbf{1}} & \beta\hat{\mathbf{1}} \end{pmatrix}, \tag{S16}$$

describes an effective perturbed system surrounded by the unperturbed homogeneous medium. Here,

$$\hat{\mathbb{S}} = \frac{1}{\sqrt{\Delta}}\begin{pmatrix} \alpha\hat{\mathbf{1}} & i\delta\hat{\mathbf{1}} \\ -i\gamma\hat{\mathbf{1}} & \beta\hat{\mathbf{1}} \end{pmatrix},$$

is the transformation matrix, and $\hat{\boldsymbol{\varepsilon}}(k,\mathbf{r})$, $\hat{\boldsymbol{\mu}}(k,\mathbf{r})$, and $\hat{\boldsymbol{\eta}}(k,\mathbf{r})$ are, respectively, the permittivity, permeability, and bi-anisotropy tensors of the optical system, which are generally inhomogeneous, anisotropic, and frequency-dependent. They are combined in Eq. (S16) into a generalized permittivity tensor $\hat{\mathbb{P}}_0(k,\mathbf{r})$, which is further used below.

Let us assume that we know the resonant states (RSs) of an optical system described by tensors $\hat{\boldsymbol{\varepsilon}}$, $\hat{\boldsymbol{\mu}}$, and $\hat{\boldsymbol{\eta}}$, and surrounded by a medium with isotropic ε_{b_0}, μ_{b_0} and η_{b_0}. Now, if these parameters of the medium are perturbed to, respectively, ε_b, μ_b, and η_b, we transform Maxwell's equations according to Eqs. (S9), (S10), and (S11), bringing the perturbed medium back to the unperturbed one at the cost of changing the system to an effective one, which is described by the generalized permittivity tensor $\tilde{\hat{\mathbb{P}}}$ given by Eq. (S16). In other words, by introducing the perturbation of the surrounding medium, we effectively modify the system itself, and therefore can apply the standard dispersive RSE [S1, S2] for treating the perturbation

$$\Delta\hat{\mathbb{P}}(\tilde{k},\mathbf{r}) = \tilde{\hat{\mathbb{P}}}(\Gamma\tilde{k},\mathbf{r}) - \hat{\mathbb{P}}_0(\tilde{k},\mathbf{r}) \tag{S17}$$

which is nonzero only within the optical system. Note that the transformed Maxwell's equations Eq. (S15) present a nonlinear eigenvalue problem for $\tilde{k}$. Expanding within the system volume the transformed electro-magnetic field $\tilde{\vec{\mathbb{F}}}$ of a perturbed RS with the wave number k_ν (transformed to $\tilde{k}$) into a complete set of the RSs of the unperturbed system,

$$\tilde{\vec{\mathbb{F}}} = \hat{\mathbb{S}}^{\dagger}\vec{\mathbb{F}}_\nu = \sum_n c_n\vec{\mathbb{F}}_n\,, \tag{S18}$$

the nonlinear Eq. (S15) is then mapped onto a linear matrix eigenvalue problem,

$$(\tilde{k}-k_n)c_n = -\tilde{k}\sum_m V_{nm}(\infty)c_m + k_n\sum_m\left[V_{nm}(\infty) - V_{nm}(k_n)\right]c_m\,, \tag{S19}$$

where the matrix elements of the perturbation are given by

$$V_{nm}(k) = \int \vec{\mathbb{F}}_n(\mathbf{r})\cdot\Delta\hat{\mathbb{P}}(k,\mathbf{r})\vec{\mathbb{F}}_m(\mathbf{r})d\mathbf{r}\,, \tag{S20}$$

in which $\Delta\hat{\mathbb{P}}(k,\mathbf{r})$, defined by Eq. (S17), is used for $k = k_n$ and $k = \infty$. In this way, the standard dispersive RSE, originally valid only for perturbations within the system, is now used for finding the RSs of an optical system in a modified (perturbed) environment surrounding it.

A. Non-chiral medium

In the case of a non-chiral medium, one just has $\eta_b = \eta_{b_0} = 0$, so that we find from Eq. (S12) a set of simultaneous equations

$$\varepsilon_{b_0} = \frac{\Gamma}{\Delta}\left(\alpha^2\varepsilon_b + \gamma^2\mu_b\right), \tag{S21}$$

$$\mu_{b_0} = \frac{\Gamma}{\Delta}\left(\delta^2\varepsilon_b + \beta^2\mu_b\right), \tag{S22}$$

$$0 = \alpha\delta\varepsilon_b + \gamma\beta\mu_b, \tag{S23}$$

which has a general solution (with $\Gamma > 0$):

$$\Gamma = \sqrt{\frac{\varepsilon_{b_0}}{\varepsilon_b}\frac{\mu_{b_0}}{\mu_b}}, \qquad \frac{\delta}{\gamma} = \sqrt{\frac{\mu_b\mu_{b_0}}{\varepsilon_b\varepsilon_{b_0}}}, \qquad \frac{\beta}{\alpha} = \sqrt{\frac{\varepsilon_b}{\varepsilon_{b_0}}\frac{\mu_{b_0}}{\mu_b}}. \tag{S24}$$

One can take a simple special case of Eq. (S24):

$$\alpha = \sqrt{\frac{\varepsilon_{b_0}}{\varepsilon_b}}, \qquad \beta = \sqrt{\frac{\mu_{b_0}}{\mu_b}}, \qquad \gamma = 0, \qquad \delta = 0, \tag{S25}$$

leading to a transformation

$$k_\nu = \Gamma\tilde{k}, \qquad \mathbf{E}_\nu(\mathbf{r}) = \alpha\tilde{\mathbf{E}}, \qquad \mathbf{H}_\nu(\mathbf{r}) = \beta\tilde{\mathbf{H}}, \tag{S26}$$

and an effective generalized permittivity within the system volume

$$\tilde{\hat{\mathbb{P}}}(k,\mathbf{r}) = \begin{pmatrix} \hat{\boldsymbol{\varepsilon}}(k,\mathbf{r})\varepsilon_{b_0}/\varepsilon_b & \hat{\boldsymbol{\eta}}(k,\mathbf{r})\Gamma \\ \hat{\boldsymbol{\eta}}^*(k,\mathbf{r})\Gamma & \hat{\boldsymbol{\mu}}(k,\mathbf{r})\mu_{b_0}/\mu_b \end{pmatrix}, \tag{S27}$$

which are used in the main text for $\hat{\boldsymbol{\eta}} = 0$.

Note that the general transformation introduced at the beginning of Sec. S.I for a bi-isotropic or chiral medium would work only if the unperturbed medium is chiral, i.e. if $\eta_{b_0} \neq 0$.

B. Frequency dispersion of the optical system and the surrounding medium

The dispersive RSE equation (S19) is based on the assumption that the frequency dispersion of the system is described by a generalized Drude-Lorentz model [S1–S3],

$$\hat{\mathbb{P}}_0(k,\mathbf{r}) = \hat{\mathbb{P}}_\infty(\mathbf{r}) + \sum_j \frac{\hat{\mathbb{Q}}_j(\mathbf{r})}{k - \Omega_j}, \tag{S28}$$

where $\hat{\mathbb{P}}_\infty(\mathbf{r})$ is the high-frequency value of the generalized permittivity, Ω_j are its simple-pole positions in the complex wave number plane, and $-i\hat{\mathbb{Q}}_j(\mathbf{r})$ are the corresponding generalized

conductivities. Overall, Eq. (S28) presents a Mittag-Leffler representation of $\hat{\mathbb{P}}_0(k, \mathbf{r})$ treated as a function of a complex variable k.

Clearly, the perturbation Eq. (S17), which includes the transformation of the wave number Eq. (S10), contains both the original poles at $\tilde{k} = \Omega_j$ of the unperturbed system in the second term of Eq. (S17) and shifted poles at $\tilde{k} = \Omega_j/\Gamma$ in the first term. One therefore has to apply the infinitesimal-dispersive RSE introduced in [S4], which requires including in the RSE basis new pole RSs. The latter are however dependent on the perturbation through the scaling factor Γ. This could make using the RSE potentially inefficient, as the infinitesimal-pole basis states have to be recalculated again and again, every time when the perturbation (i.e. the properties of the surrounding medium) changes. In order to avoid this complication, we have introduced a simple transformation of the original pole modes of the basis system which produces an alternative set of basis states replacing the new pole RSs. This transformation does not require calculating new basis states every time but instead uses the same fixed set of states of the basis system, by simply re-scaling them in space. This is described in more detail in Sec. S.IV. below and illustrated there numerically on an example of a Drude model of gold.

Let us finally note that if any of the parameters describing the surrounding medium, such as $\varepsilon_b(k)$, $\mu_b(k)$, and $\eta_b(k)$, as well as $\varepsilon_{b_0}(k)$, $\mu_{b_0}(k)$, and $\eta_{b_0}(k)$, depend on the wave number k, the general transformation method would not work. This can be easily seen for a non-magnetic and non-chiral medium, in which case

$$\Gamma(k, k_\nu) = \sqrt{\frac{\varepsilon_{b_0}(k)}{\varepsilon_b(k_\nu)}} \tag{S29}$$

becomes state-dependent, as it explicitly depends on k_ν and is thus different for different states.

Nevertheless, dispersive surrounding media can be treated by means of RS regularization as described in Sec. S.II C below, leading to analytic results which in first order coincide with those reported in [S5], as demonstrated in Sec. S.II D.

C. First-order approximation

Now we would like to obtain from the RSE a first order approximation in terms of the perturbation parameters, keeping in the expression for the perturbed RSs wave number k_ν only terms linear in δ_ε, δ_μ, and δ_η, where

$$\delta_\varepsilon = \varepsilon_b/\varepsilon_{b_0} - 1\,, \qquad \delta_\mu = \mu_b/\mu_{b_0} - 1\,, \qquad \delta_\eta = \eta_b/\eta_{b_0} - 1\,. \tag{S30}$$

To do this, we first consider the diagonal version of the RSE equation (S19), for clarity of presentation assuming non-chiral environment ($\eta_b = \eta_{b_0} = 0$):

$$\frac{k_\nu}{k_n} \approx \frac{n_{b_0}}{n_b} \frac{1 + V_{nn}(\infty) - V_{nn}(k_n)}{1 + V_{nn}(\infty)}\,. \tag{S31}$$

Noting that $\varepsilon_{b_0}/\varepsilon_b \approx 1-\delta_\varepsilon$ and $\mu_{b_0}/\mu_b \approx 1-\delta_\mu$, as well as

$$\Gamma = \frac{n_{b_0}}{n_b} \approx 1 - \frac{1}{2}\left(\delta_\varepsilon + \delta_\mu\right) , \tag{S32}$$

calculated to first order, and taking into account that in this limit $V_{nn}(\infty)$ is linear in δ_ε and δ_μ, we find from Eq. (S31)

$$\frac{k_\nu}{k_n} \approx 1 - V_{nn}(k_n) - \frac{1}{2}\left(\delta_\varepsilon + \delta_\mu\right) . \tag{S33}$$

Let us now evaluate $V_{nn}(k_n)$ to first order. The permittivity perturbation contributing to $V_{nn}(k_n)$ has the form [see Eq. (S17)]:

$$\Delta\hat{\boldsymbol{\varepsilon}}(\tilde{k},\mathbf{r}) = \hat{\boldsymbol{\varepsilon}}(k,\mathbf{r})\frac{\varepsilon_{b_0}}{\varepsilon_b} - \hat{\boldsymbol{\varepsilon}}(\tilde{k},\mathbf{r}) , \tag{S34}$$

where $\tilde{k} = k/\Gamma = k_n$, from what we find

$$k - k_n = k_n(\Gamma - 1) \approx -\frac{k_n}{2}(\delta_\varepsilon + \delta_\mu) , \tag{S35}$$

to first order. Expanding also to first order $\hat{\boldsymbol{\varepsilon}}(k,\mathbf{r}) \approx \hat{\boldsymbol{\varepsilon}}(k_n,\mathbf{r}) + \hat{\boldsymbol{\varepsilon}}'(k_n,\mathbf{r})(k-k_n)$, where the prime means the derivative with respect to k, we find

$$\Delta\hat{\boldsymbol{\varepsilon}}(k_n,\mathbf{r}) \approx -\hat{\boldsymbol{\varepsilon}}(k_n,\mathbf{r})\delta_\varepsilon - \hat{\boldsymbol{\varepsilon}}'(k_n,\mathbf{r})\frac{k_n}{2}(\delta_\varepsilon + \delta_\mu) . \tag{S36}$$

Similarly,

$$\Delta\hat{\boldsymbol{\mu}}(k_n,\mathbf{r}) \approx -\hat{\boldsymbol{\mu}}(k_n,\mathbf{r})\delta_\mu - \hat{\boldsymbol{\mu}}'(k_n,\mathbf{r})\frac{k_n}{2}(\delta_\varepsilon + \delta_\mu) . \tag{S37}$$

Introducing integrals over the system volume $\mathcal{V}_{\text{in}}$,

$$I^E_{nm} = \int_{\mathcal{V}_{\text{in}}} \mathbf{E}_n \cdot \hat{\boldsymbol{\varepsilon}}(k_n,\mathbf{r})\mathbf{E}_m d\mathbf{r}, \qquad J^E_n = k_n \int_{\mathcal{V}_{\text{in}}} \mathbf{E}_n \cdot \hat{\boldsymbol{\varepsilon}}'(k_n,\mathbf{r})\mathbf{E}_n d\mathbf{r} , \tag{S38}$$

$$I^H_{nm} = \int_{\mathcal{V}_{\text{in}}} \mathbf{H}_n \cdot \hat{\boldsymbol{\mu}}(k_n,\mathbf{r})\mathbf{H}_m d\mathbf{r}, \qquad J^H_n = k_n \int_{\mathcal{V}_{\text{in}}} \mathbf{H}_n \cdot \hat{\boldsymbol{\mu}}'(k_n,\mathbf{r})\mathbf{H}_n d\mathbf{r} , \tag{S39}$$

the diagonal matrix element of the perturbation takes the form

$$V_{nn}(k_n) \approx -I^E_{nn}\delta_\varepsilon + I^H_{nn}\delta_\mu + (-J^E_n + J^H_n)\frac{1}{2}(\delta_\varepsilon + \delta_\mu) , \tag{S40}$$

so that finally

$$\frac{k_n - k_\nu}{k_n} \approx \frac{1}{2}\left(1 - 2I^E_{nn} - J^E_n + J^H_n\right)\delta_\varepsilon + \frac{1}{2}\left(1 + 2I^H_{nn} - J^E_n + J^H_n\right)\delta_\mu . \tag{S41}$$

It is convenient, for the purpose of comparison with other approaches which is done in the following section, to introduce

$$A_n = I^E_{nn} + J^E_n - I^H_{nn} - J^H_n , \qquad B_n = I^E_{nn} + I^H_{nn} , \tag{S42}$$

so that Eq. (S41) can be written as

$$\frac{k_n - k_\nu}{k_n} \approx \frac{1 - A_n}{2}(\delta_\varepsilon + \delta_\mu) - \frac{B_n}{2}(\delta_\varepsilon - \delta_\mu) . \tag{S43}$$

Clearly, for non-dispersive systems $J^E_n = J^H_n = 0$, and A_n simplifies to $A_n = I^E_{nn} - I^H_{nn}$.

S.II. TREATING EXTERNAL PERTURBATIONS BY REGULARIZATION

In this section, we introduce an alternative approach to the calculation of perturbations of the RSs of an arbitrary optical system due to changes of the surrounding medium. This approach is based on regularization of RS wave functions.

To regularize them, Zel'dovich proposed [S6] to multiply all the RS wave functions with a Gaussian factor $e^{-\alpha r^2}$ and take the limit $\alpha \to +0$ after integration. This allows one to extend the integration in the volume term of the analytic normalization to the entire space and drop the vanishing surface term. This yields exactly to the same normalization as the analytic rigorous normalization, as has been recently demonstrated in [S7] for the RSs of a homogeneous dielectric sphere. Alternatives to this regularization are the complex coordinate transformation [S8] and use of perfectly matched layers [S9, S10], ideally leading to the same result for the RS norm.

Applying any valid regularization to the RS field, such as a Gaussian regularization introduced by Zel'dovich [S6], or the one imposed by a perfectly matched layer (PML) [S10], on can see that both the RS normalization and orthogonality then take the form of a scalar product, similar to those of a Hermitian system [S11]. However, a completeness of such regularized RSs in the full space is still not achievable, as demonstrated in Sec. S.II E below. We note, however, that completeness can in principle be achieved by adding to the regularized physical RSs an additional set of numerical modes [S11] formed due to imperfections of perfectly matched layers and spatial discretization of the wave equation. These modes are, however, fully unphysical, i.e. they do not exist in reality in the physical system and are an artifact of a numerical calculation. We also note that the present approach does not use any perfectly matched layers or spatial discretization of Maxwell's equations.

In this section, the idea of regularization of the RSs allows us to develop an alternative valuable approximation (see Sec. S.II C), which is similar to the full diagonal approximation Eq. (S31), but as we demonstrate below on various examples, is not as accurate as Eq. (S31).

A. Orthonormality of resonant states and Poynting's theorem

The general analytic normalization of the (unperturbed) RSs has the form [S1]:

$$\int_{\mathcal{V}} \vec{\mathbb{F}}_n(\mathbf{r}) \cdot \left[k\hat{\mathbb{P}}_0(k,\mathbf{r})\right]' \vec{\mathbb{F}}_n(\mathbf{r}) d\mathbf{r} + i \oint_{\mathcal{S}} \left(\mathbf{E}_n \times \mathbf{H}'_n - \mathbf{E}'_n \times \mathbf{H}_n\right) \cdot d\mathbf{S} = 1\,, \tag{S44}$$

where $\mathcal{V}$ is an arbitrary volume including all inhomogeneities of the generalized permittivity $\hat{\mathbb{P}}_0(k,\mathbf{r})$, $\mathcal{S}$ is the outer boundary of $\mathcal{V}$, the prime means the derivative with respect to k taken at $k = k_n$, and $\mathbf{E}'_n$ and $\mathbf{H}'_n$ are the derivatives of an analytic continuation of the RS fields in the complex k-plane.

The orthogonality of the RSs has a similar form [S12, S13]:

$$\int_{\mathcal{V}} \vec{\mathbb{F}}_n(\mathbf{r}) \cdot \left[k_n\hat{\mathbb{P}}_0(k_n,\mathbf{r}) - k_m\hat{\mathbb{P}}_0(k_m,\mathbf{r})\right] \vec{\mathbb{F}}_m(\mathbf{r}) d\mathbf{r} + i \oint_{\mathcal{S}} (\mathbf{E}_m \times \mathbf{H}_n - \mathbf{E}_n \times \mathbf{H}_m) \cdot d\mathbf{S} = 0 \tag{S45}$$

for $n \neq m$. Note that in deriving Eq. (S45), the reciprocity of the system was used: $\hat{\mathbb{P}}_0^{\mathrm{T}}(k,\mathbf{r}) = \hat{\mathbb{P}}_0(k,\mathbf{r})$, where T denotes the matrix transpose.

Poynting's theorem for the RSs fields in reciprocal systems takes the following form [S1]:

$$\int_{\mathcal{V}} \left[\mathbf{E}_n(\mathbf{r}) \cdot k_n \hat{\boldsymbol{\varepsilon}}(k_n,\mathbf{r})\mathbf{E}_m(\mathbf{r}) + \mathbf{H}_n(\mathbf{r}) \cdot k_m \hat{\boldsymbol{\mu}}(k_m,\mathbf{r})\mathbf{H}_m(\mathbf{r})\right] d\mathbf{r} + i \oint_{\mathcal{S}} \mathbf{E}_m \times \mathbf{H}_n \cdot d\mathbf{S} = 0\,, \quad \text{(S46)}$$

valid for both cases of $n \neq m$ and $n = m$.

It is easy to see that subtracting from Eq. (S46) the same equation in which n and m are swapped results in the RS orthogonality Eq. (S45).

B. Orthonormality and Poynting's theorem for regularized resonant states

For regularized RSs, the volume integration in Eqs. (S44), (S45), and (S46) can be extended to the *entire space*. Then all the surface integrals vanish since the regularized fields tend to zero at infinity. This results in the following form of the normalization condition

$$\int \vec{\mathbb{F}}_n(\mathbf{r}) \cdot \left[k\hat{\mathbb{P}}_0(k,\mathbf{r})\right]' \vec{\mathbb{F}}_n(\mathbf{r}) d\mathbf{r} = 1\,, \quad \text{(S47)}$$

orthogonality

$$k_n \int \vec{\mathbb{F}}_n(\mathbf{r}) \cdot \hat{\mathbb{P}}_0(k_n,\mathbf{r}) \vec{\mathbb{F}}_m(\mathbf{r}) d\mathbf{r} = k_m \int \vec{\mathbb{F}}_n(\mathbf{r}) \cdot \hat{\mathbb{P}}_0(k_m,\mathbf{r}) \vec{\mathbb{F}}_m(\mathbf{r}) d\mathbf{r}\,, \quad \text{(S48)}$$

and Poynting's theorem

$$k_n \int \mathbf{E}_n(\mathbf{r}) \cdot \hat{\boldsymbol{\varepsilon}}(k_n,\mathbf{r})\mathbf{E}_m(\mathbf{r}) d\mathbf{r} = -k_m \int \mathbf{H}_n(\mathbf{r}) \cdot \hat{\boldsymbol{\mu}}(k_m,\mathbf{r})\mathbf{H}_m(\mathbf{r}) d\mathbf{r}\,, \quad \text{(S49)}$$

where the integration of the regularized fields is performed over the entire space. Note that a proper regularization of the RS wave functions not only makes the integrals in Eqs. (S47), (S48), and (S49) finite but also the field normalization converging to the exact general normalization given by Eq. (S44).

For non-dispersive systems and non-dispersive surrounding materials, the orthonormality given by Eqs. (S47) and (S48) simplifies to

$$\int \vec{\mathbb{F}}_n(\mathbf{r}) \cdot \hat{\mathbb{P}}_0(\mathbf{r}) \vec{\mathbb{F}}_m(\mathbf{r}) d\mathbf{r} = \delta_{nm}\,, \quad \text{(S50)}$$

where δ_{nm} is the Kronecker symbol. Moreover, with the help of Poynting's theorem Eq. (S49), the electric and magnetic fields can be separated which results in two equivalent expressions for the RS orthonormality:

$$2\int \mathbf{E}_n(\mathbf{r}) \cdot \hat{\boldsymbol{\varepsilon}}(\mathbf{r})\mathbf{E}_m(\mathbf{r}) d\mathbf{r} = \delta_{nm}\,, \qquad 2\int \mathbf{H}_n(\mathbf{r}) \cdot \hat{\boldsymbol{\mu}}(\mathbf{r})\mathbf{H}_m(\mathbf{r}) d\mathbf{r} = -\delta_{nm}\,. \quad \text{(S51)}$$

Now, going back to dispersive systems and combining the orthonormality Eqs. (S47) and (S48) and Poynting's theorem Eq. (S49), one can express the integrals over the infinite exterior volume,

$$W_{nm}^{E} = \int_{\mathcal{V}_{\rm out}} \mathbf{E}_n \cdot \mathbf{E}_m d\mathbf{r}\,, \qquad W_{nm}^{H} = \int_{\mathcal{V}_{\rm out}} \mathbf{H}_n \cdot \mathbf{H}_m d\mathbf{r}\,, \tag{S52}$$

in term of those over the system volume. In fact, using the integrals defined by Eqs. (S38), (S39), and (S52), the RS normalization Eq. (S47) can be written as

$$A_n + [k\varepsilon_{b_0}(k)]' W_{nn}^{E} - [k\mu_{b_0}(k)]' W_{nn}^{H} = 1\,, \tag{S53}$$

where again the frequency derivatives are taken at $k = k_n$, and A_n is defined in Eq. (S42). The Poynting theorem Eq. (S49) in turns takes the form

$$k_n[I_{nm}^{E} + \varepsilon_{b_0}(k_n) W_{nm}^{E}] = -k_m[I_{mn}^{H} + \mu_{b_0}(k_m) W_{mn}^{H}]\,. \tag{S54}$$

Using Eq. (S54) for $n = m$ and combining it with the normalization Eq. (S53) we obtain:

$$W_{nn}^{E} = \frac{(1-A_n)\mu_{b_0} - B_n(k\mu_{b_0})'}{(k\varepsilon_{b_0})'\mu_{b_0} + (k\mu_{b_0})'\varepsilon_{b_0}}\,, \tag{S55}$$

$$W_{nn}^{H} = \frac{-(1-A_n)\varepsilon_{b_0} - B_n(k\varepsilon_{b_0})'}{(k\varepsilon_{b_0})'\mu_{b_0} + (k\mu_{b_0})'\varepsilon_{b_0}}\,, \tag{S56}$$

where the arguments of $\varepsilon_{b_0}(k)$ and $\mu_{b_0}(k)$ are omitted for brevity, and B_n is defined in Eq. (S42).

For $n \neq m$, we write the orthogonality Eq. (S48) as

$$k_n[I_{nm}^{E} - I_{nm}^{H} + \varepsilon_{b_0}(k_n) W_{nm}^{E} - \mu_{b_0}(k_n) W_{nm}^{H}] = k_m[I_{mn}^{E} - I_{mn}^{H} + \varepsilon_{b_0}(k_m) W_{mn}^{E} - \mu_{b_0}(k_m) W_{mn}^{H}]\,. \tag{S57}$$

Using the symmetry $W_{nm}^{E,H} = W_{mn}^{E,H}$ (which does not hold in general for other integrals, i.e. $I_{nm}^{E,H} \neq I_{mn}^{E,H}$), we obtain

$$W_{nm}^{E} = -\frac{k_n^2\mu_{b_0}(k_n) I_{nm}^{E} - k_m^2\mu_{b_0}(k_m) I_{mn}^{E} + k_n k_m[\mu_{b_0}(k_n) I_{mn}^{H} - \mu_{b_0}(k_m) I_{nm}^{H}]}{k_n^2\varepsilon_{b_0}(k_n)\mu_{b_0}(k_n) - k_m^2\varepsilon_{b_0}(k_m)\mu_{b_0}(k_m)}\,, \tag{S58}$$

$$W_{nm}^{H} = -\frac{k_n^2\varepsilon_{b_0}(k_n) I_{nm}^{H} - k_m^2\varepsilon_{b_0}(k_m) I_{mn}^{H} + k_n k_m[\varepsilon_{b_0}(k_n) I_{mn}^{E} - \varepsilon_{b_0}(k_m) I_{nm}^{E}]}{k_n^2\varepsilon_{b_0}(k_n)\mu_{b_0}(k_n) - k_m^2\varepsilon_{b_0}(k_m)\mu_{b_0}(k_m)}\,. \tag{S59}$$

Finally, for non-dispersive permittivity and permeability, the orthonormality Eq. (S51) can be written as

$$I_{nm}^{E} + \varepsilon_{b_0} W_{nm}^{E} = \frac{1}{2}\delta_{nm}\,, \qquad I_{nm}^{H} + \mu_{b_0} W_{nm}^{H} = -\frac{1}{2}\delta_{nm}\,, \tag{S60}$$

which can also be used as a link between the integrals $W_{nm}^{E,H}$ of the electric and magnetic fields over the infinite volume $\mathcal{V}_{\rm out}$ of the space surrounding the system and the integrals $I_{nm}^{E,H}$ over the finite volume $\mathcal{V}_{\rm in}$ containing the system. Clearly, Eq. (S60) is a special (non-dispersive) case of Eqs. (S55) and (S56) for $n = m$ and of Eqs. (S58) and (S59) for $n \neq m$.

C. Regularized diagonal approximation

To derive the diagonal approximation for perturbations of the regularized RSs due to changes in the surrounding medium, we allow the unperturbed medium to be different from vacuum and also to have a frequency dispersion.

The Maxwell equations for the unperturbed RSs are given by

$$\left[k_n\hat{\mathbb{P}}_0(k_n,\mathbf{r})-\hat{\mathbb{D}}(\mathbf{r})\right]\vec{\mathbb{F}}_n(\mathbf{r})=0\,, \tag{S61}$$

which is the same equation as Eq. (1) of the main text, but $\hat{\mathbb{P}}_0(k_n,\mathbf{r})$ now includes arbitrary homogeneous isotropic and frequency dispersive permittivity $\varepsilon_{b_0}(k)$ and permeability $\mu_{b_0}(k)$ of the surrounding medium. Perturbed RSs satisfy Eq. (3) of the main text, here written as

$$\left[k_\nu\hat{\mathbb{P}}_0(k_\nu,\mathbf{r})+k_\nu\delta\hat{\mathbb{P}}(k_\nu,\mathbf{r})-\hat{\mathbb{D}}(\mathbf{r})\right]\vec{\mathbb{F}}_\nu(\mathbf{r})=0\,, \tag{S62}$$

where the perturbation $\delta\hat{\mathbb{P}}(k,\mathbf{r})$ consists of only changes of the permittivity and permeability of the surrounding medium, given, respectively, by $\varepsilon_b(k)-\varepsilon_{b_0}(k)=\varepsilon_{b_0}(k)\delta_\varepsilon$ and $\mu_b(k)-\mu_{b_0}(k)=\mu_{b_0}(k)\delta_\mu$, in accordance with Eq. (S30). Now using the diagonal approximation for the wave function, $\vec{\mathbb{F}}_\nu(\mathbf{r})\approx\vec{\mathbb{F}}_n(\mathbf{r})$, Eq. (S62) becomes

$$\left[k_\nu\hat{\mathbb{P}}_0(k_\nu,\mathbf{r})-k_n\hat{\mathbb{P}}_0(k_n,\mathbf{r})+k_\nu\delta\hat{\mathbb{P}}(k_\nu,\mathbf{r})\right]\vec{\mathbb{F}}_n(\mathbf{r})\approx 0\,, \tag{S63}$$

in which the term $\hat{\mathbb{D}}(\mathbf{r})\vec{\mathbb{F}}_n(\mathbf{r})$ was excluded with the help of Eq. (S61). For small changes of the wave numbers, $|k_\nu-k_n|\ll|k_n|$, one can Taylor expand the generalized permittivity in Eq. (S63) as

$$k_\nu\hat{\mathbb{P}}_0(k_\nu,\mathbf{r})\approx k_n\hat{\mathbb{P}}_0(k_n,\mathbf{r})+(k_\nu-k_n)\left[k\hat{\mathbb{P}}_0(k,\mathbf{r})\right]'\,, \tag{S64}$$

so that Eq. (S63) becomes

$$\left[(k_\nu-k_n)\left[k\hat{\mathbb{P}}_0(k,\mathbf{r})\right]'+k_\nu\delta\hat{\mathbb{P}}(k_\nu,\mathbf{r})\right]\vec{\mathbb{F}}_n(\mathbf{r})\approx 0\,. \tag{S65}$$

Multiplying it with $\vec{\mathbb{F}}_n(\mathbf{r})$ and integrating over the entire space, we obtain

$$(k_\nu-k_n)+k_\nu\int\vec{\mathbb{F}}_n(\mathbf{r})\cdot\delta\hat{\mathbb{P}}(k_\nu,\mathbf{r})\vec{\mathbb{F}}_n(\mathbf{r})d\mathbf{r}\approx 0\,, \tag{S66}$$

where we have used the normalization condition Eq. (S47). Finally, neglecting the difference between k_ν and k_n in the perturbation $\delta\hat{\mathbb{P}}$, results in the following explicit expression for the perturbed RS wave numbers in the diagonal approximation:

$$\frac{k_n}{k_\nu}\approx 1+W^E_{nn}\varepsilon_{b_0}(k_n)\delta_\varepsilon-W^H_{nn}\mu_{b_0}(k_n)\delta_\mu\,. \tag{S67}$$

D. First-order approximation and comparison with Both&Weiss [S5].

From Eq. (S67) follows immediately the first-order approximation:

$$\frac{k_n - k_\nu}{k_n} \approx W^E_{nn}\varepsilon_{b_0}(k_n)\delta_\varepsilon - W^H_{nn}\mu_{b_0}(k_n)\delta_\mu\,. \tag{S68}$$

For a non-dispersive surrounding medium, it coincides with Eq. (S43) obtained from the RSE in first order. In fact, if both ε_{b_0} and μ_{b_0} have no dispersion, Eqs. (S55) and (S56) simplify to

$$W^E_{nn} = \frac{1 - A_n - B_n}{2\varepsilon_{b_0}}\,, \qquad W^H_{nn} = \frac{-1 + A_n - B_n}{2\mu_{b_0}}\,, \tag{S69}$$

in accordance with Eq. (S60), and Eqs. (S43) and (S68) become identical. For a dispersive surrounding medium, Eq. (S68) can be written more explicitly, using Eqs. (S55) and (S56), as

$$\frac{k_n - k_\nu}{k_n} \approx \frac{(1 - A_n)\varepsilon_{b_0}\mu_{b_0}(\delta_\varepsilon + \delta_\mu) - B_n\left[(k\mu_{b_0})'\varepsilon_{b_0}\delta_\varepsilon - (k\varepsilon_{b_0})'\mu_{b_0}\delta_\mu\right]}{(k\varepsilon_{b_0})'\mu_{b_0} + (k\mu_{b_0})'\varepsilon_{b_0}}\,, \tag{S70}$$

where again all values are taken at $k = k_n$.

Let us now compare Eq. (S70) with the first-order results presented in [S5]. The latter is given by

$$k_\nu \approx k_n - \frac{k_n\left\langle \mathbb{F}_n \left| \delta\hat{\mathbb{P}}\,(k_n) \right| \mathbb{F}_n \right\rangle + S}{\left\langle \mathbb{F}_n \left| (k\hat{\mathbb{P}})' \right| \mathbb{F}_n \right\rangle + \left[\mathbb{F}_n \mid \mathbb{F}'_n\right]} \tag{S71}$$

where

$$\left\langle \mathbb{F}_n \left| (k\hat{\mathbb{P}})' \right| \mathbb{F}_n \right\rangle = \int_{\mathcal{V}_{in}} \left[\mathbf{E}_n(\mathbf{r}) \cdot (k\hat{\boldsymbol{\varepsilon}})'\,\mathbf{E}_n(\mathbf{r}) - \mathbf{H}_n(\mathbf{r}) \cdot (k\hat{\boldsymbol{\mu}})'\,\mathbf{H}_n(\mathbf{r})\right] d\mathbf{r} \tag{S72}$$

and

$$\left[\mathbb{F}_n \mid \mathbb{F}'_n\right] = \oint_{\mathcal{S}_{in}} \left(\mathbf{E}_n \times \mathbf{H}'_n - \mathbf{E}'_n \times \mathbf{H}_n\right) \cdot d\mathbf{S}\,, \tag{S73}$$

with $\mathcal{S}_{in}$ being the outer surface of $\mathcal{V}_{in}$.

The first term in the numerator of Eq. (S71) vanishes as there is no perturbation within the system, while the second term S represents the perturbation in the region outside it. According to [S5], it is given by

$$S = \bar{\eta}\frac{k_n}{2}(\delta_\varepsilon + \delta_\mu)\left[\mathbb{F}_n \mid \mathbb{F}'_n\right] + \frac{i}{2}\bar{\eta}\left[\frac{(k\mu_{b_0})'}{\mu_{b_0}}\delta_\varepsilon - \frac{(k\varepsilon_{b_0})'}{\varepsilon_{b_0}}\delta_\mu\right]\oint_{\mathcal{S}_{in}} (\mathbf{E}_n \times \mathbf{H}_n) \cdot d\mathbf{S} \tag{S74}$$

with

$$\bar{\eta} = \frac{\sqrt{\varepsilon_{b_0}\mu_{b_0}}}{(k\sqrt{\varepsilon_{b_0}\mu_{b_0}})'} = \frac{2\varepsilon_{b_0}\mu_{b_0}}{(k\varepsilon_{b_0})'\mu_{b_0} + (k\mu_{b_0})'\varepsilon_{b_0}}\,. \tag{S75}$$

Using the RS normalization Eq. (S44), the first surface integral in Eq. (S74) can be expressed as

$$\left[\mathbb{F}_n \mid \mathbb{F}'_n\right] = 1 - \left\langle \mathbb{F}_n \left| (k\hat{\mathbb{P}})' \right| \mathbb{F}_n \right\rangle = 1 - A_n\,. \tag{S76}$$

This also entirely removes from Eq. (S71) the denominator, since the latter is equal to 1. The second surface integral in Eq. (S74) can, in turn, be expressed as

$$\frac{i}{k_n}\oint_{\mathcal{S}_{in}} \cdot (\mathbf{E}_n \times \mathbf{H}_n)\, d\mathbf{S} = -\int_{\mathcal{V}in} \left[\mathbf{E}_n(\mathbf{r}) \cdot \hat{\boldsymbol{\varepsilon}}\mathbf{E}_n(\mathbf{r}) + \mathbf{H}_n(\mathbf{r}) \cdot \hat{\boldsymbol{\mu}}\mathbf{H}_n(\mathbf{r})\right] d\mathbf{r} = -B_n\,, \tag{S77}$$

using the Poyting theorem Eq. (S46) for $n = m$ [see Eq. (S42) for the definition of A_n and B_n]. This makes Eq. (S71) identical to the first-order result Eq. (S70) obtained for regularized RSs.

E. Lack of completeness of regularized states

The success of using regularized RSs for treating perturbations of the medium surrounding an optical system is demonstrated above in this section. It is therefore natural to consider also a hypothesis that the regularized RSs may be complete not only within the system volume (as the RSs themselves) but also outside it. Below we check this hypothesis by using the regularized states as a basis for expansion of perturbed regularized RSs in the region outside the system, again assuming both unperturbed and perturbed media homogeneous and isotropic. We also consider for simplicity the case of both the system and the medium being non-dispersive. Without dispersion, regularized RSs satisfy the orthonormality relation Eq. (S50).

Assuming the regularized RSs are complete in the entire space, let us expand the fields of a perturbed (regularized) RS as

$$\vec{\mathbb{F}}_\nu(\mathbf{r}) = \sum_n \bar{c}_n \vec{\mathbb{F}}_n(\mathbf{r})\,. \tag{S78}$$

Using Eq. (S78) and Maxwell's equations for the basis RSs,

$$\left[k_n\hat{\mathbb{P}}_0(\mathbf{r}) - \hat{\mathbb{D}}(\mathbf{r})\right]\vec{\mathbb{F}}_n(\mathbf{r}) = 0\,, \tag{S79}$$

we solve the perturbed Maxwell's equations

$$\left[k_\nu\hat{\mathbb{P}}_0(\mathbf{r}) + k_\nu\delta\hat{\mathbb{P}}(\mathbf{r}) - \hat{\mathbb{D}}(\mathbf{r})\right]\vec{\mathbb{F}}_\nu(\mathbf{r}) = 0\,, \tag{S80}$$

where k_ν is the wave number of the perturbed state ν and $\delta\hat{\mathbb{P}}(\mathbf{r})$ is the perturbation of the generalized permittivity. Substituting Eq. (S78) into Eq. (S80) and using Eq. (S79), we find

$$\sum_n \bar{c}_n \left[(k_\nu - k_n)\hat{\mathbb{P}}_0(\mathbf{r}) + k_\nu\delta\hat{\mathbb{P}}(\mathbf{r})\right]\vec{\mathbb{F}}_n(\mathbf{r}) = 0\,. \tag{S81}$$

Multiplying the last equation with $\vec{\mathbb{F}}_m(\mathbf{r})$, integrating over the entire space, and using the orthonormality Eq. (S50), we end up with a matrix eigenvalue problem,

$$\bar{c}_n(k_\nu - k_n) + k_\nu\sum_m \bar{V}_{nm}\bar{c}_m = 0\,, \tag{S82}$$

where

$$\bar{V}_{nm} = \int \vec{\mathbb{F}}_n(\mathbf{r}) \cdot \delta\hat{\mathbb{P}}(\mathbf{r})\vec{\mathbb{F}}_m(\mathbf{r})d\mathbf{r} \tag{S83}$$

are the matrix elements of the perturbation.

To verify the regularized matrix equation (S82) we consider the transverse-electric (TE) RSs of a dielectric sphere with permittivity $\varepsilon = 4$, surrounded by vacuum ($\varepsilon_{b_0} = 1$) which is perturbed to a non-magnetic medium with permittivity $\varepsilon_b = 2$. The spectra of the unperturbed and perturbed TE modes with the orbital momentum $l = 1$ are compared in Fig. S1(a). The perturbed RSs are calculated exactly and via the regularized Eq. (S82)

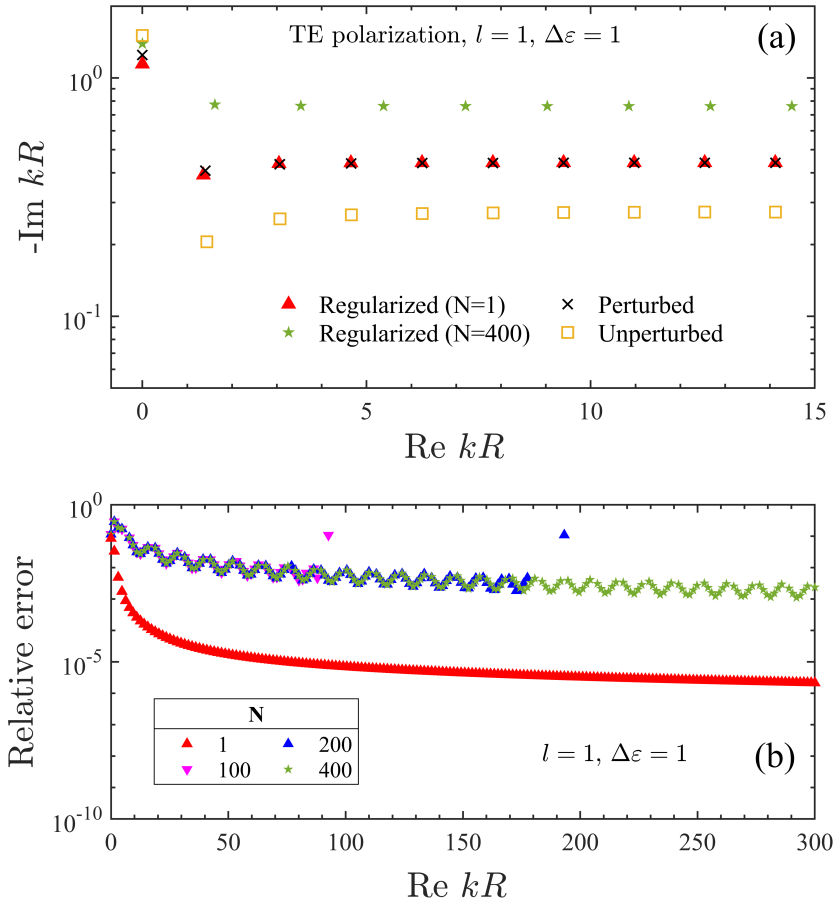

FIG. S1. (a) Exact unperturbed (squares) and perturbed (crosses) RS wave numbers of a dielectric sphere ($\varepsilon = 4$) in vacuum, perturbed to a non-magnetic surrounding medium with $\varepsilon_b = 2$, for TE polarization and $l = 1$. The perturbed wave numbers are calculated either by solving the exact analytic secular equation (S88) for a sphere ($\times$) or by solving the regularized matrix equation (S82) [equivalent to Eq. (S85)] with the total number of basis states $N = 400$ (stars) and $N = 1$ (triangles). (b) Relative errors for the wave numbers calculated via Eq. (S82) with different N as given.

truncated to $N = 400$ basis states. Figure S1(a) demonstrates an obvious difference between the exact and 'regularized' wave numbers for this rather large perturbation of the medium ($\Delta\varepsilon = \varepsilon_b - \varepsilon_{b_0} = 1$). Furthermore, the relative error in Fig. S1(b) shown for $N = 100$, 200, and 400 clearly demonstrates that the wave numbers calculated via Eq. (S82) do not converge to the exact values as N increases. This is a clear evidence that Eq. (S78) is not valid outside the system. In other words, the RSs, even regularized, are not complete outside the system. Interestingly, the first-order approximation still works. Moreover, the diagonal approximation, i.e. the use of Eq. (S82) with $n = m$ (corresponding to $N = 1$) produces a lot better result than any $N > 1$, see Fig. S1.

To see how the RSE-based approach works for the same example, we show in Fig. S2 a comparison of the RSE and exact results for the same parameters as in Fig. S1, demonstrating a quick convergence to the exact solution, with the relative error scaling as $1/N^3$, typical for the RSE.

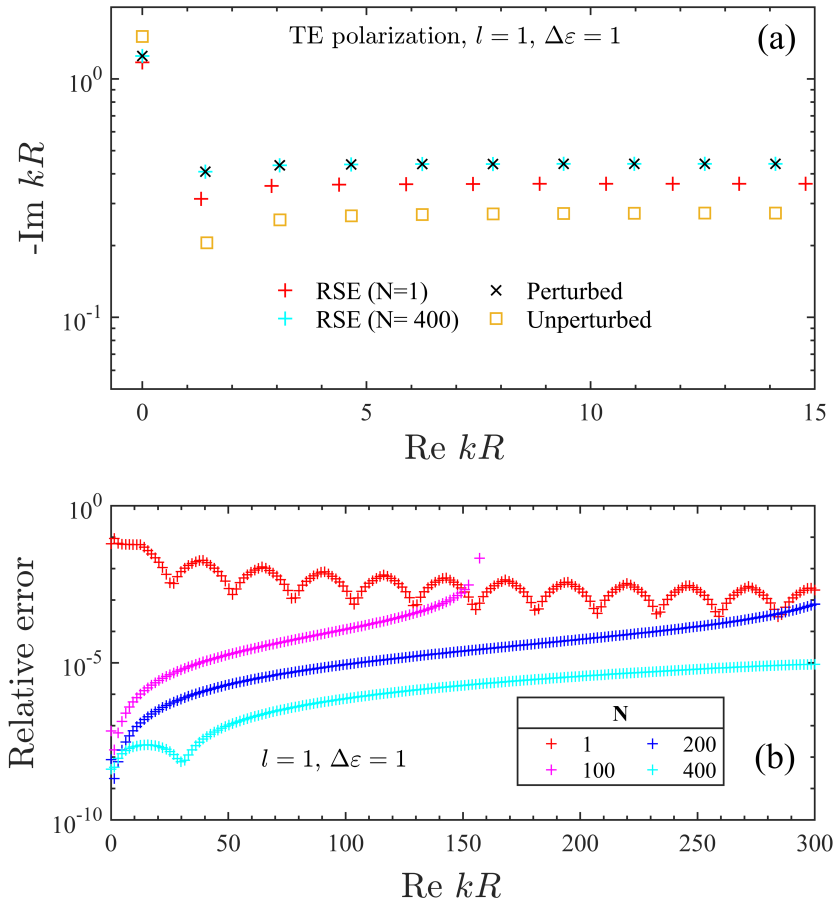

FIG. S2. As Fig. S1 but with the regularized solution replaced with the solution of the RSE equation (S19) [taking the form of Eq. (S86) for non-dispersive systems].

The difference between the RSE Eq. (S19) and regularized Eq. (S82) can be clearly seen also on the analytical level, by bringing both equations to the same format. Let us first transform the matrix elements in Eq. (S82), expressing them in terms of the field integrals over the system region. Using the perturbation $\delta\hat{\mathbb{P}}(\mathbf{r}) = \left[(\varepsilon_b - \varepsilon_{b_0})\,\hat{\mathbf{1}}; (\mu_b - \mu_{b_0})\,\hat{\mathbf{1}}\right]$ for $\mathbf{r} \in \mathcal{V}_{\rm out}$ and $\delta\hat{\mathbb{P}}(\mathbf{r}) = 0$ for $\mathbf{r} \in \mathcal{V}_{\rm in}$, we find

$$\bar{V}_{nm} = (\varepsilon_b - \varepsilon_{b_0}) W^E_{nm} - (\mu_b - \mu_{b_0}) W^H_{nm}\,, \tag{S84}$$

where $W^{E,H}_{nm}$ are defined by Eq. (S52). For non-dispersive permittivity and permeability, they can be expressed, using the orthonormality Eq. (S60), in terms of the integrals $I^{E,H}_{nm}$ over the system volume, which are defined by Eqs. (S38) and (S39). The matrix equation (S82) then takes the form

$$k_\nu \sum_m \left[\frac{\delta_{nm}}{2} \left(\frac{\varepsilon_b}{\varepsilon_{b_0}} + \frac{\mu_b}{\mu_{b_0}} \right) + \frac{\varepsilon_b}{\varepsilon_{b_0}} \left(\frac{\varepsilon_{b_0}}{\varepsilon_b} - 1 \right) I^E_{nm} - \frac{\mu_{b_0}}{\mu_b} \left(\frac{\mu_b}{\mu_{b_0}} - 1 \right) I^H_{nm} \right] \bar{c}_m = k_n \bar{c}_n\,. \tag{S85}$$

On the other hand, the RSE equation (S19) for the same non-dispersive system and an effective perturbation $\Delta\hat{\mathbb{P}}(\mathbf{r}) = \left[\left(\varepsilon_{b_0}/\varepsilon_b - 1\right)\hat{\boldsymbol{\varepsilon}}(\mathbf{r}); \left(\mu_{b_0}/\mu_b - 1\right)\hat{\boldsymbol{\mu}}(\mathbf{r})\right]$ for $\mathbf{r} \in \mathcal{V}_{\rm in}$ and $\Delta\hat{\mathbb{P}}(\mathbf{r}) = 0$ for $\mathbf{r} \in \mathcal{V}_{\rm out}$, which describes the same changes of the surrounding material, can be written as

$$k_\nu \sum_m \sqrt{\frac{\varepsilon_b}{\varepsilon_{b_0}} \frac{\mu_b}{\mu_{b_0}}} \left[\delta_{nm} + \left(\frac{\varepsilon_{b_0}}{\varepsilon_b} - 1 \right) I^E_{nm} - \left(\frac{\mu_b}{\mu_{b_0}} - 1 \right) I^H_{nm} \right] c_m = k_n c_n\,, \tag{S86}$$

by using the transformation of the perturbed wave number Eq. (S26) and the matrix elements of the effective perturbation

$$V_{nm} = \left(\frac{\varepsilon_{b_0}}{\varepsilon_b} - 1 \right) I^E_{nm} - \left(\frac{\mu_b}{\mu_{b_0}} - 1 \right) I^H_{nm}\,. \tag{S87}$$

There is an obvious difference between Eqs. (S85) and (S86), even in the diagonal approximation. However, it can be easily seen that they agree in first order, which is also observed in the numerics.

S.III. SECULAR EQUATION FOR THE RESONANT STATES OF A HOMOGENEOUS SPHERE IN A MEDIUM, THEIR WAVE FUNCTIONS AND ANALYTIC NORMALIZATION

Let us consider an optical resonator in a form of a sphere surrounded by a medium, with the material both inside and outside the sphere being homogeneous, isotropic and generally frequency dispersive. The permittivity (permeability) of such an optical system is given by step-like functions in the radial direction, taking values ε (μ) and ε_b (μ_b), respectively,

inside and outside the sphere, all four quantities having in general a frequency dispersion. The continuity of the tangent components of the electric and magnetic fields results in the following transcendental secular equation for the RSs of the sphere:

$$\beta^{(p)} J'(n_r z) H(n_b z) = J(n_r z) H'(n_b z)\,, \tag{S88}$$

see e.g. [S13] for derivation. Here, $J(x) = x j_l(x)$ and $H(x) = x h_l^{(1)}(x)$, where $j_l(x)$ and $h_l^{(1)}(x)$ are, respectively, the spherical Bessel function and Hankel function of first kind, primes mean the derivatives of functions with respect to their arguments, $z = k_n R$, k_n is the RS wave number, R is the sphere radius, $n_b = \sqrt{\varepsilon_b \mu_b}$ and $n_r = \sqrt{\varepsilon(k_n)\mu(k_n)}$ are the refractive indices of, respectively, the surrounding medium and the sphere, (p) is the polarization of light (TE or TM), and $\beta^{\mathrm{TE}} = \beta$ for TE and $\beta^{\mathrm{TM}} = 1/\beta$ for transverse-magnetic (TM) polarization, where

$$\beta = \sqrt{\frac{\varepsilon(k_n)}{\varepsilon_b}\frac{\mu_b}{\mu(k_n)}}\,. \tag{S89}$$

Below we focus on the nonmagnetic case only (i.e. with $\mu = \mu_b = 1$), arbitrary dispersive $\varepsilon(k)$ and non-dispersive ε_b. The permittivity in the entire space is then described by

$$\epsilon(k, r) = \begin{cases} n_r^2(k) & \text{for } r \leqslant R\,, \\ n_b^2 & \text{for } r > R\,. \end{cases} \tag{S90}$$

Using spherical coordinates $\mathbf{r} = (r, \theta, \varphi)$, the electric field of the RSs in TM polarization is given by [S14]

$$\mathbf{E}_n^{\mathrm{TM}}(k_n, \mathbf{r}) = \frac{A_{nl}}{\epsilon(k_n, r) k_n r} \begin{pmatrix} l(l+1) R_l(k_n, r) Y_{lm} \\ \frac{\partial}{\partial r}\left(r R_l\left(k_n, r\right)\right) \frac{\partial}{\partial \theta} Y_{lm}(\theta, \varphi) \\ \frac{\partial}{\partial r}\left(r R_l\left(k_n, r\right)\right) \frac{1}{\sin\theta} \frac{\partial}{\partial \varphi} Y_{lm}(\theta, \varphi) \end{pmatrix}, \tag{S91}$$

where Y_{lm} are the spherical harmonics and R_l are the radial functions defined as

$$R_l(k_n, r) = \begin{cases} \frac{j_l(n_r k_n r)}{j_l(n_r k_n R)} & \text{for } r \leqslant R\,, \\ \frac{h_l^{(1)}(n_b k_n r)}{h_l^{(1)}(n_b k_n R)} & \text{for } r > R\,. \end{cases} \tag{S92}$$

The wave functions are normalized according to Eq. (S44), which yields

$$\frac{1}{[A_{nl}]^2} = l(l+1) R^3 (n_r^2 - n_b^2) D_{nl}\,, \tag{S93}$$

where

$$D_{nl} = \frac{1}{n_r^2}\left[\frac{j_{l-1}(z)}{j_l(z)} - \frac{l}{z}\right]^2 + \frac{l(l+1)}{n_b^2 z^2} + \eta C_{nl} \tag{S94}$$

and C_{nl} satisfies the equation

$$(n_r^2 - n_b^2)C_{nl} = -\frac{2l}{z^2} + \frac{j_{l-1}^2(z)}{j_l^2(z)} - \frac{j_{l-2}(z)}{j_l(x)}\,, \tag{S95}$$

with $z = n_r k_n R$ and $n_r = n_r(k_n)$. The factor η takes the dispersion into account,

$$\eta = \frac{k}{2\varepsilon(k)} \frac{\partial \varepsilon(k)}{\partial k}\bigg|_{k=k_n}\,, \tag{S96}$$

and is vanishing for non-dispersive systems. One can see that for $n_b = 1$, the analytical normalization of the TM RSs presented in [S4, S15] is reproduced.

S.IV. EFFECTIVE POLE RESONANT STATES FOR INFINITESIMAL DISPERSIVE RSE

As already mentioned in Sec. S.I B, the transformation Eq. (S10) of the wave number leads in dispersive systems to a shift of the pole positions in the permittivity or permeability, which in turn results in a need of introducing degenerate pole RSs (pRSs), see [S4] for the definition. This may potentially lead to an inefficiency of applying the RSE to systems with gradual changes of the environment, since every time when the environment is changed, the pRSs have to be recalculated for a changed position of the permittivity (permeability) pole. To mitigate this complication, we introduce here an alternative approach based on a simple, good quality approximation in which the true pRSs are replaced with some effective pRSs generated by the unperturbed permittivity.

For the purpose of illustration of the above idea, we focus in this section on a relatively simple example of a spherical non-magnetic nanoparticle in vacuum with the dispersion described by the Drude model,

$$\varepsilon(k) = \varepsilon_\infty + \frac{i\sigma}{k} - \frac{i\sigma}{k - \Omega} \tag{S97}$$

with the Drude pole at $k = \Omega$, where $\Omega = -i\gamma$, and γ is the Drude damping. Note that Eq. (S97) is a special case of the more general Drude-Lorentz dispersion given by Eq. (S28). According to [S4], pRSs for the dispersion Eq. (S97) are found by taking the limit $\xi \to 0$ both in the conductivity $-i\sigma = \xi$ and the in mode wave number $k_m = \Omega + \xi q_m$, where the index m is used to label the pRS. The quantum numbers q_m are finite and are related to effective permittivities ε_m of the pRSs, according to

$$\varepsilon_m = \varepsilon_\infty + \frac{1}{q_m}\,, \tag{S98}$$

for the Drude dispersion Eq. (S97). Note that while all pRS are degenerate, i.e. $k_m = \Omega$, different pRSs have different values of q_m and consequently ε_m. The latter determine the

spatial distribution of the pRS fields within the basis system while the former contribute to their normalisation, see [S4] for details.

To find the eigen permittivities ε_m, one needs to solve Eq. (S88) for n_r while fixing the mode frequency at $k_m = \Omega$. For a spherical Drude nanoparticle in vacuum, Eq. (S88) leads to

$$n_r J'(n_r z)H(z) = J(n_r z)H'(z) \qquad \text{(TE)} \tag{S99}$$

for TE polarization, with the eigenvalues $n_r = \sqrt{\varepsilon_m^{\mathrm{TE}}}$, and to

$$\frac{1}{n_r} J'(n_r z)H(z) = J(n_r z)H'(z) \qquad \text{(TM)} \tag{S100}$$

for TM polarization, with the eigenvalues $n_r = \sqrt{\varepsilon_m^{\mathrm{TM}}}$, and $z = \Omega R$ fixed in both equations.

According to Eqs. (S16) and (S17), the perturbed permittivity has the form

$$\tilde{\varepsilon}(k) = \varepsilon(k\Gamma)\Gamma^2\,, \tag{S101}$$

where $\Gamma = 1/\sqrt{\varepsilon_b}$ and ε_b is the permittivity of the background medium, here assumed for simplicity non-magnetic and non-dispersive. The modified permittivity $\tilde{\varepsilon}(k)$ of the effective perturbed system in vacuum therefore has a Drude pole shifted to $k = \tilde{\Omega} = \Omega\sqrt{\varepsilon_b}$. The pRSs due to $\tilde{\varepsilon}(k)$ are given (again taking the limit $\sigma \to 0$) by a modified secular equation

$$\tilde{n}_r J'(\tilde{n}_r \tilde{z})H(\tilde{z}) = J(\tilde{n}_r \tilde{z})H'(\tilde{z}) \qquad \text{(TE)} \tag{S102}$$

with $\tilde{n}_r = \sqrt{\tilde{\varepsilon}_m^{\mathrm{TE}}}$ for TE polarization, and

$$\frac{1}{\tilde{n}_r} J'(\tilde{n}_r \tilde{z})H(\tilde{z}) = J(\tilde{n}_r \tilde{z})H'(\tilde{z}) \qquad \text{(TM)} \tag{S103}$$

with $\tilde{n}_r = \sqrt{\tilde{\varepsilon}_m^{\mathrm{TM}}}$ for TM polarization. In other words, the new eigenvalues, $\tilde{\varepsilon}_m^{\mathrm{TE}}$ and $\tilde{\varepsilon}_m^{\mathrm{TM}}$, are found by solving Eqs. (S102) and (S103) for a fixed value of $\tilde{z} = \tilde{\Omega}R = \sqrt{\varepsilon_b}\Omega R$. Clearly, Eqs. (S102) and (S103) have to be solved again and again, every time when background permittivity ε_b changes. However, for small $\tilde{z}$ (for example, $\tilde{z}$ is of order of 10^{-3} for a gold nanosphere of radius $R = 10\,\mathrm{nm}$), one can approximate $H'(z)/H(z) \approx -l/z$, so that Eq. (S102) simplifies to

$$\tilde{n}_r \tilde{z} J'(\tilde{n}_r \tilde{z}) \approx -l J(\tilde{n}_r \tilde{z}) \qquad \text{(TE)}\,, \tag{S104}$$

which is equivalent, in the same approximation, to Eq. (S99), provided that $\tilde{n}_r = n_r/\sqrt{\varepsilon_b}$. Therefore,

$$\tilde{\varepsilon}_m^{\mathrm{TE}} \approx \frac{\varepsilon_m^{\mathrm{TE}}}{\varepsilon_b}\,. \tag{S105}$$

Applying the same approximation to TM polarization, Eq. (S103) simplifies to

$$\frac{\tilde{z}}{\tilde{n}_r} J'(\tilde{n}_r \tilde{z}) \approx -l J(\tilde{n}_r \tilde{z}) \qquad \text{(TM)}\,, \tag{S106}$$

which does not seem to be equivalent to Eq. (S100). However, since $|z| \ll 1$ both Eqs. (S100) and (S106) are well approximated by

$$j_l(\tilde{n}_r \tilde{z}) \approx j_l(n_r z) \approx 0 \qquad \text{(TE \& TM)}\,, \tag{S107}$$

actually working equally well for both polarizations, so that again

$$\tilde{\varepsilon}_m^{\mathrm{TM}} \approx \frac{\varepsilon_m^{\mathrm{TM}}}{\varepsilon_b} \approx \frac{1}{\varepsilon_b}\left(\frac{Z_{l,m}^{\mathrm{Bess}}}{\Omega R}\right)^2 \quad \text{for } m > 0\,, \tag{S108}$$

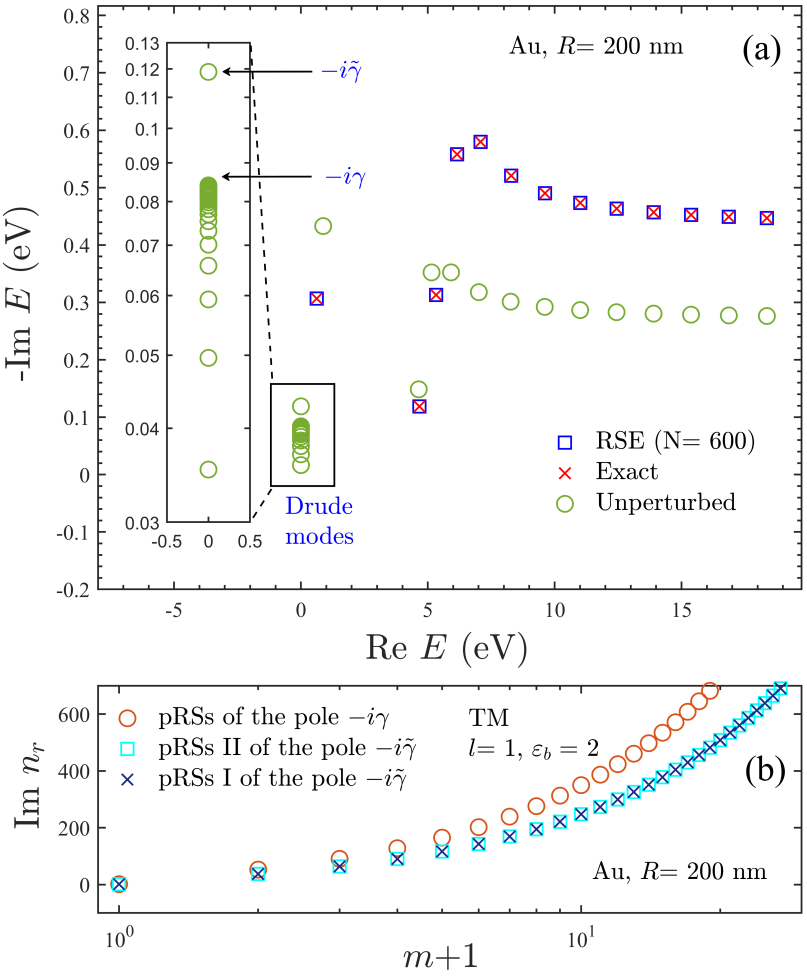

FIG. S3. (a) As Fig.1 of the main text but with the RSE calculation using pRSs II and an inset showing accumulation of the basis RSs around the unperturbed Drude pole, as well as the perturbed Drude pole generating pRSs. (b) Values of the refractive index of the pRSs as function of the mode number m, for the unperturbed pole at $k = -i\gamma$ (red circles) and for the perturbed pole at $k = -i\tilde{\gamma} = -i\gamma\sqrt{\varepsilon_b}$ of the Drude dispersion. For the shifted Drude pole, the refractive index for the pRSs is calculated exactly (pRSs I, blue crosses) and using the approximation Eqs. (S105), (S108), and (S109) (pRSs II, blue squares).

where $Z_{l,m}^{\mathrm{Bess}}$ is the m-th root of the spherical Bessel function $j_l(Z)$. However, the fundamental pRS in TM polarization, $m = 0$, has to be treated separately, namely by approximating also $J'(z)/J(z) \approx (l+1)/z$ at small z. This yields

$$\tilde{\varepsilon}_{m=0}^{\mathrm{TM}} \approx \varepsilon_{m=0}^{\mathrm{TM}} \approx -\frac{l+1}{l}\,, \tag{S109}$$

which is formally the same equation as for the localized surface plasmon (SP) in a spherical nanoparticle in the electrostatic limit, see e.g. Eq. (B9) in [S4]. Clearly, Eq. (S109) implies that the lowest-order pRS can be taken the same as in the unperturbed system.

To summarize, the approximate basis of pRSs (further called pRSs II) introduced above is calculated from the unperturbed basis of pRSs, satisfying Eqs. (S99) and (S100), by using simple relations between their eigen permittivities Eqs. (S105) and (S108), with the exception for the fundamental pRS in TM polarization, which is instead calculated according to Eq. (S109). The unperturbed eigen permittivities ε_m in both polarizations can also be found from the roots of the Bessel functions, in accordance with Eqs. (S107) and (S108). The approximate basis of pRSs II is then used to replace the exact basis of pRSs (further called pRSs I) satisfying Eqs. (S102) and (S103). We note that even though the eigen permittivities ε_m are found with a limited accuracy, more important is the completeness of the full set of basis functions used in the RSE, supplemented with either pRSs I or pRSs II, both

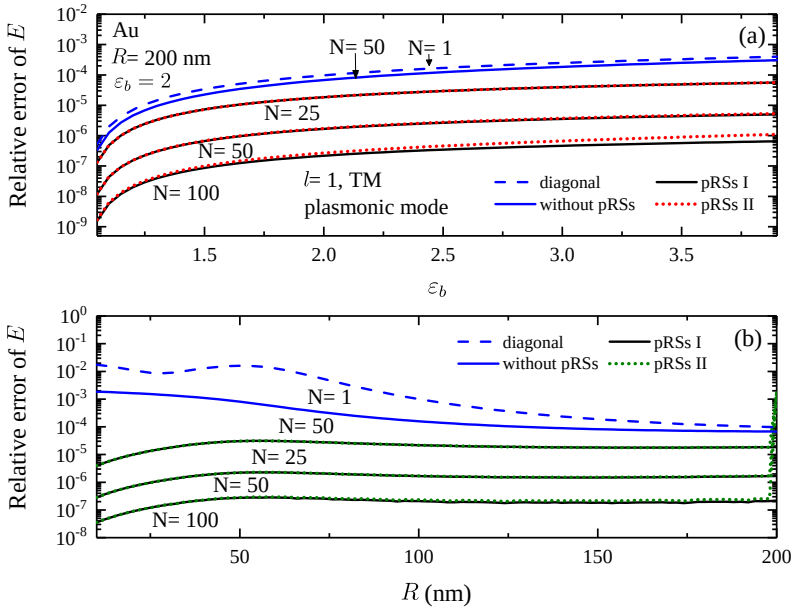

FIG. S4. Relative error for the wave numbers of the fundamental (dipolar, $l = 1$) plasmonic mode of a gold nanosphere as function of the permittivity ε_b of the surrounding medium, calculated by the RSE with pRSs I (black solid lines) and pRSs II (red and green dotted lines) for $N = 50$, 100 and 200, as well as without pRSs ($N = 50$, solid blue lines) and in the diagonal approximation ($N = 1$, dashed blue lines).

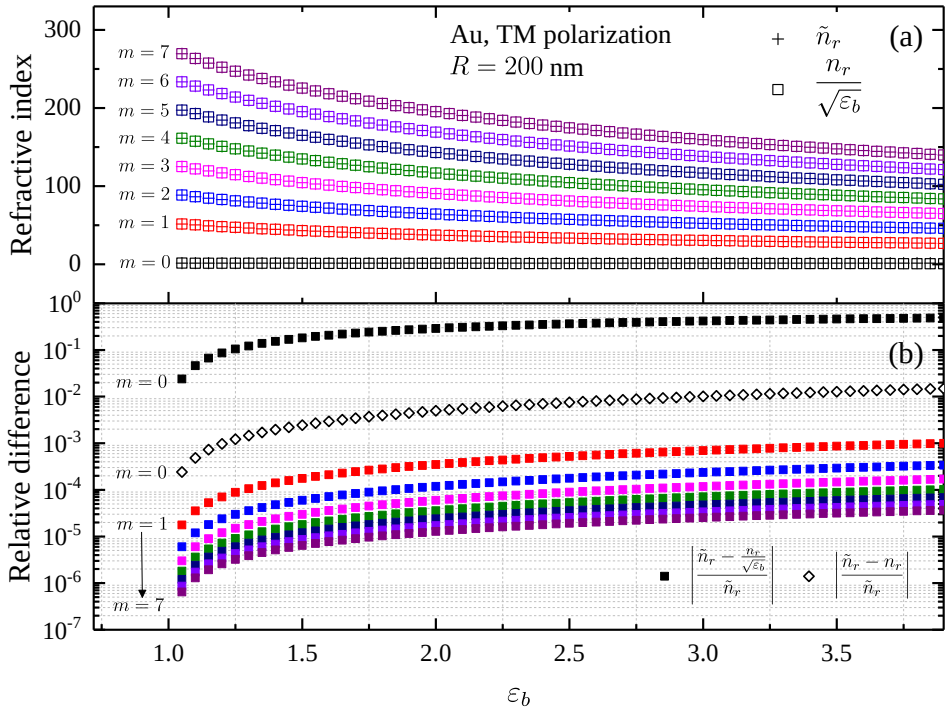

FIG. S5. (a) The imaginary part of refractive index of the first few pRSs in TM polarization of a gold nanosphere of radius $R = 200\,\text{nm}$ described by the Drude model as functions of the permittivity of the surrounding medium ε_b, calculated exactly, i.e. via Eq. (S102) ($\tilde{n}_r$, crosses), and by using the approximation Eq. (S108). (b) The relative error for the approximation Eq. (S108) (full squares) and Eq. (S109) for the lowest-order mode only (open diamonds).

providing a quick convergence to the exact solution.

In order to illustrate the above approximation, we show in Fig. S3(b) the refractive index of pRSs for the unperturbed and perturbed Drude permittivities, demonstrating a visual agreement between pRSs I and pRSs II. The RS wave numbers of a gold nanosphere in vacuum perturbed to a medium with $\varepsilon_b = 2$, calculated with the approximate set of pRSs II are presented in Fig. S3(a), again showing agreement with the exact values. Furthermore, the approximate basis of pRS II is working so well that the $1/N^3$ convergence to the exact solution, typical for the RSE (N is the basis size) is almost unaffected, as demonstrated by Fig. S4. Note that in the numerical calculation, the number of pRSs is always taken equal to the number of RSs. Without pRSs, the error for $N = 50$ basis RSs, also shown in Fig. S4, is almost the same as for the diagonal approximation ($N = 1$), i.e. keeping only the unperturbed SP mode in the basis.

We also provide in Figs. S5 and S6 a detailed comparison of the pRSs I and II, the latter given the approximations Eqs. (S108) and (S109). One can see that the values of the refractive index $\tilde{n}_r$ of the exact pRSs I (crosses) are in good visual agreement with those

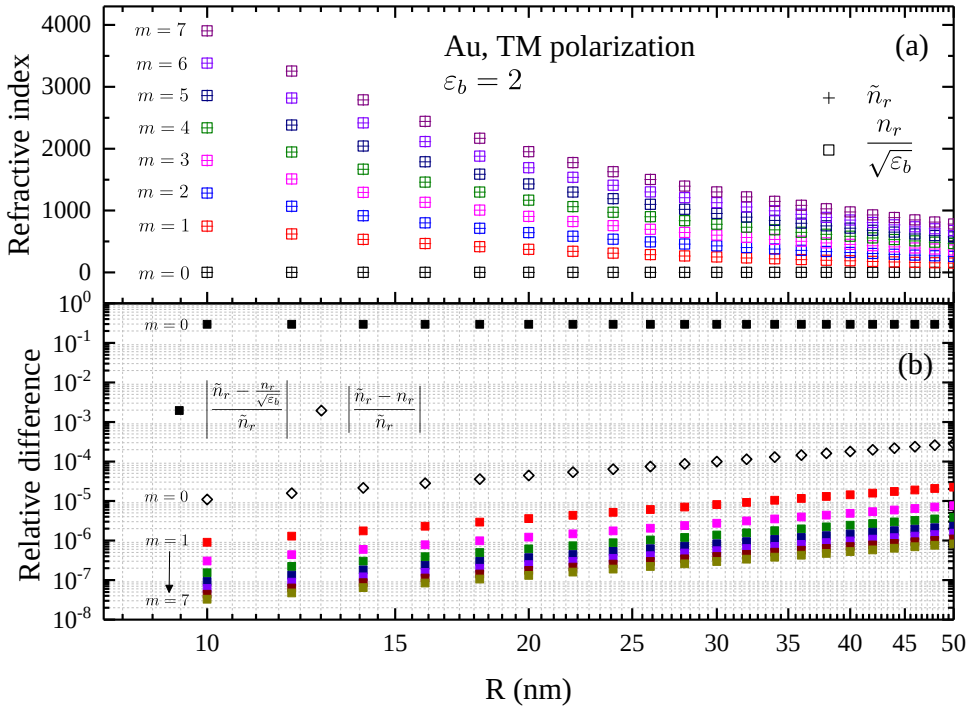

FIG. S6. As Fig. S5 but for the dependence on the sphere radius R, for $\varepsilon_b = 2$.

of the approximate pRS II given by Eq. (S108) (squares), for a wide range of values of the medium permittivity ε_b and sphere radius R, as exemplifies in Figs. S5(a) and S6(a), for the first eight pRSs. The relative error for the approximate modes presented in Figs. S5(b) and S6(b) shows, however, the weakness of this approximation for the fundamental ($m = 0$) mode. This approximation is then refined by using Eq. (S109) instead, compare the full black squares and diamonds in Figs. S5(b) and S6(b). Note that the error for all modes grows with radius [see Fig. S6(b)], in accordance with the approximation $|\tilde{\Omega}R| \ll 1$ used.

S.V. MORE RESULTS

A. Gold nanosphere: Comparison with Both&Weiss [S5]

The energy and the linewidth of the fundamental plasmonic dipolar ($l = 1$) and quadrupolar ($l = 2$) modes of a gold nanosphere of radius $R = 200\,\text{nm}$ surrounded by a dielectric medium with varying permittivity ε_b are shown in Figs. S7(a) and (b), respectively. The unperturbed system has $\varepsilon_{b_0} = 2$ of the surrounding material. This is exactly the same system as used for illustration of the first-order theory presented in [S5]. Figure S7 compares the exact solution with the first-order result, identical to [S5], with the full and diagonal RSE, as well as with the diagonal regularized approximation. We see that for the chosen

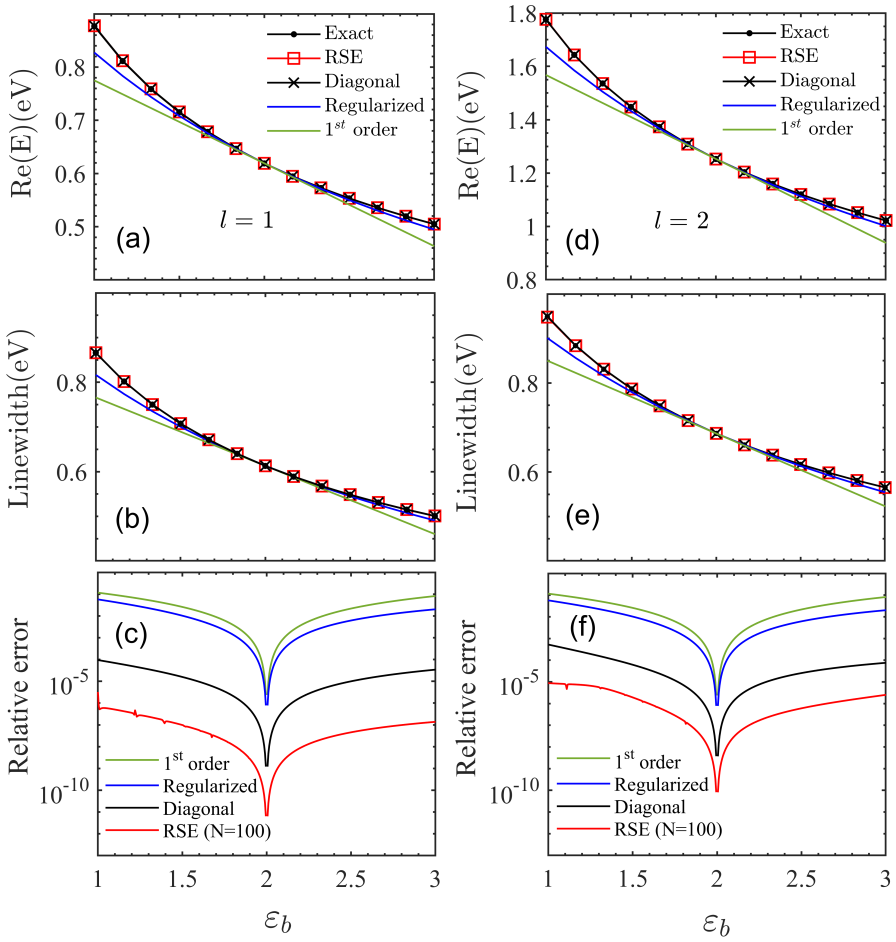

FIG. S7. Energy (a,d) and linewidth (b,d) of the fundamental plasmonic dipolar (left) and quadrupolar mode (right) of the gold nanosphere of radius $R = 200\,\mathrm{nm}$ as functions of the permittivity ε_b of the material surrounding the sphere, calculated using the full RSE with $N = 100$ basis states (red lines with squares), diagonal RSE (black lines with crosses), regularized theory (blue lines), and first-order approximation (green lines). The unperturbed system has the surrounding permittivity of $\varepsilon_{b_0} = 2$. The Drude model is using $\varepsilon_\infty = 4$ with the other parameters fitted to the Johnson&Christy data [S16] via the fit programme provided in [S3]. (c) and (f) show the corresponding relative errors compared to the exact solutions.

parameters of the unperturbed system, namely for the value of $\varepsilon_{b_0} = 2$ lying in the middle of the selected range $1 \leqslant \varepsilon_b \leqslant 3$, the first-order results are in a much better agreement with the exact solution in this range than in a similar Fig. 2 of the main text where the unperturbed system has $\varepsilon_{b_0} = 1$. Nevertheless, as it is clear from Figs. S7(c) and (f), the diagonal RSE shows a lot better agreement with the exact solution, while the full RSE is quickly converging to it with increasing the basis size. This is also illustrated in Figs. 2(c) of the main text.

B. Silica micro-sphere

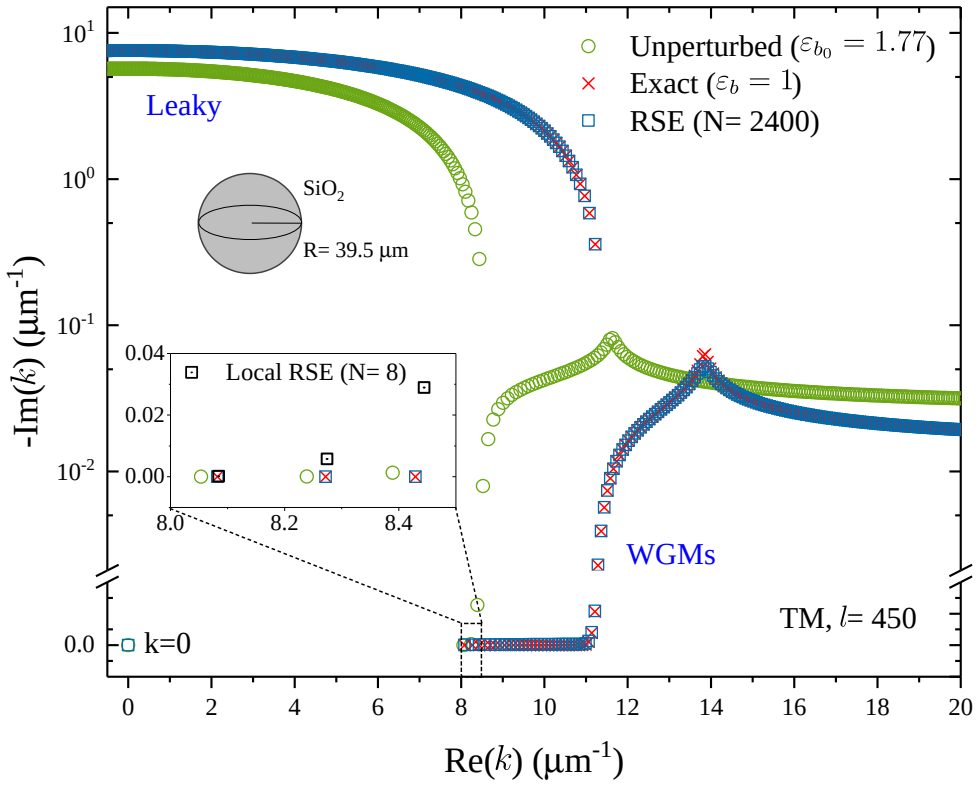

FIG. S8. Complex wave numbers k of the RSs of a silica micro-sphere of radius $R = 39.5\,\mu$m in water with $\varepsilon_{b_0} = 1.77$ (green open circles) and in vacuum, calculated with the RSE (blue squares) and analytically (red crosses), for TM polarization and $l = 450$. Inset: Local RSE (black squares with dots) with only WG modes included in the basis.

An experimentally relevant example we show here is high-angular momentum ($l = 450$) whispering gallery (WG) modes of a silica micro-sphere of radius $R = 39.5\,\mu$m [S17, S18]. For silica, the permittivity is calculated using Sellmeier formula [S18] at wavelength $\lambda = 780\,$nm, giving $\varepsilon = 2.114$. Figure S8 shows the spectra of the RSs of the silica sphere in water ($\varepsilon_{b_0} = 1.77$) and in vacuum ($\varepsilon_b = 1$) playing the role of, respectively, the basis and perturbed systems. To reach in the full RSE the relative error of 10^{-5} or below, one needs to keep $N = 2400$ states in the basis, see Fig. S9. The perturbed system has a large number of WG modes which are all well reproduced by the RSE even though the basis system has only four pairs of them. All single mode approximations fail in this case, as it is clear from Fig. S9. However, keeping only the WG modes in basis ($N = 8$) provides a very good approximation for the fundamental mode, as demonstrated by the inset of Fig. S8 and Fig. S10.

Figures S9 and S10 show the real part of wave number of the fundamental WG mode and the relative error for its calculation by various methods, including local RSE, as functions

of the permittivity ε_b of the surrounding material changing between water ($\varepsilon_b = \varepsilon_{b_0} = 1.77$, unperturbed) and vacuum ($\varepsilon_b = 1$). The relative error shown in Fig. S9(b) demonstrates a quick convergence of the RSE to the exact solution: In fact, the relative error scales with the basis size N approximately as $1/N^3$, which is the same behaviour as in all other systems treated by the RSE. However, the errors in Fig. S9(b) have larger magnitude for the same basis size compared to other examples of this work. This is due to a very low permittivity contrast in the unperturbed system which makes the resonances described by the basis RSs less pronounced. Decreasing ε_b, this permittivity contrast rapidly increases which in turn makes the basis and perturbed states very different. This explains why the single-mode (i.e. diagonal, regularized, and first-order) approximations so poorly reproduce the exact result,

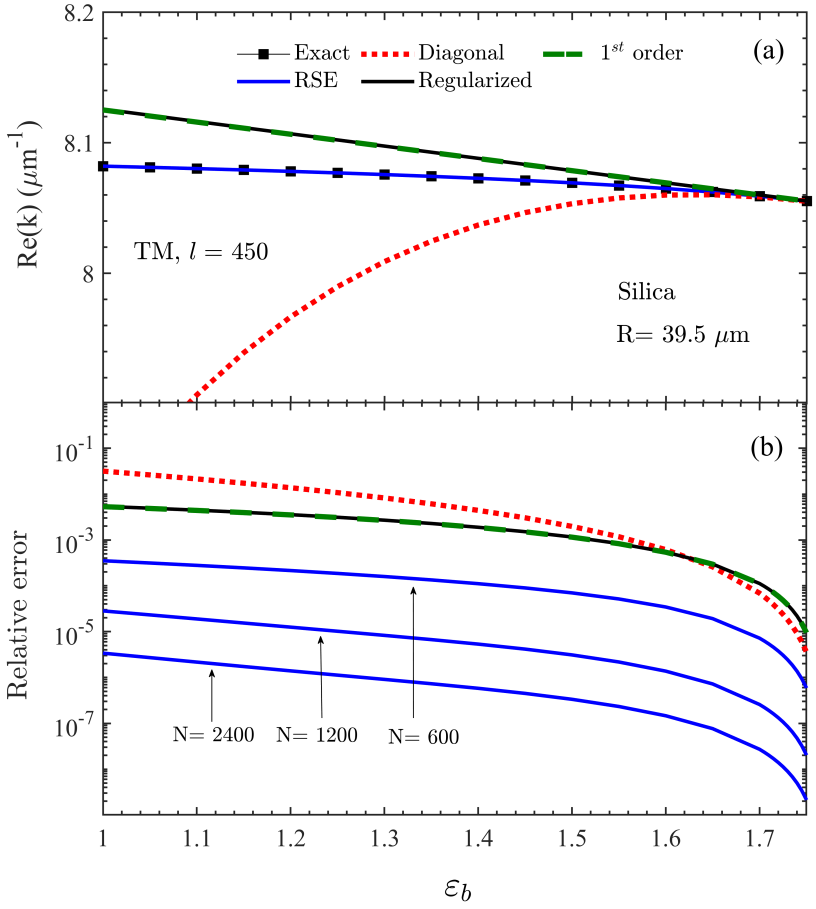

FIG. S9. (a) Real part and (b) relative error of the wave number k of the $l = 450$ TM fundamental WG mode of a silica micro-sphere as functions of the background permittivity ε_b, calculated exactly (black line with squares), using the full RSE with different basis sizes N as given, using the diagonal ($N = 1$) RSE (dotted red lines), regularized (black lines) and first-order (green lines) approximations.

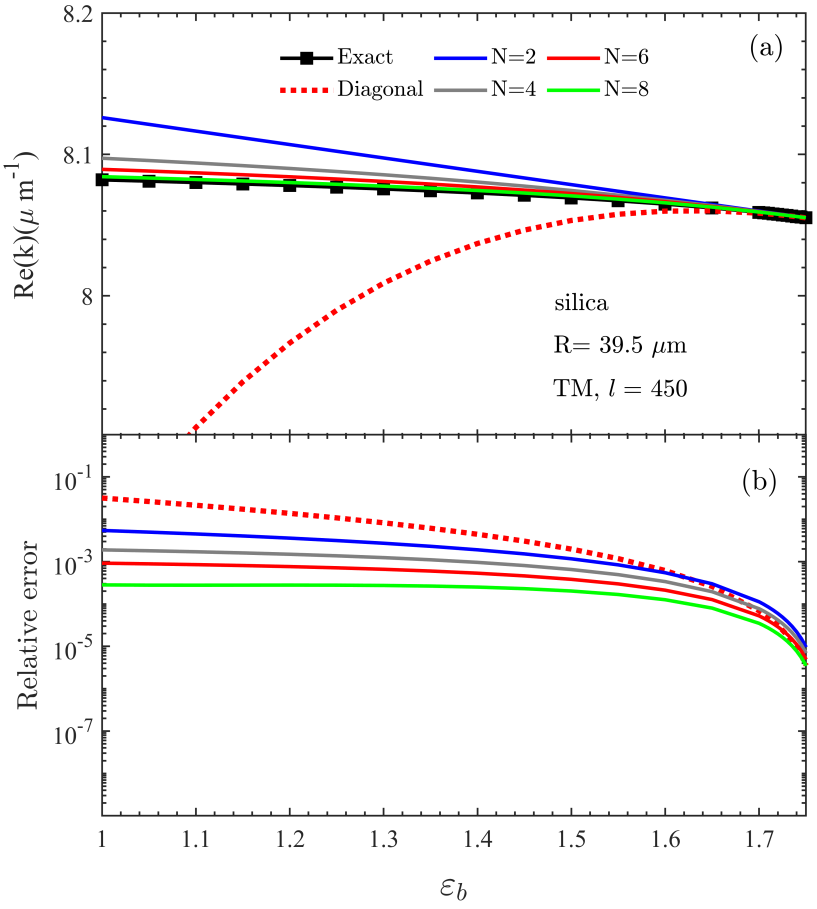

FIG. S10. As Fig. S9 but with the exact solution (black line with squares) compared with diagonal RSE ($N = 1$, dotted red lines), and local RSE with $N = 2$ (blue lines), $N = 4$ (gray lines), $N = 6$ (red solid lines), and $N = 8$ (green lines).

as we see in Fig. S9.

The poor quality of the approximations presented in Fig. S9 can be significantly improved by using the local RSE, introduced in [S14]. In the local RSE, only the RSs which are close in frequency to the state of interest or have the biggest overlap matrix elements with this state are kept in the basis. This was controlled in [S14] by introducing weights $W = |V_{nm}^2/(k_n - k_m)|$ proportional to the second-order correction to the inverse wave number, in accordance with the Rayleigh-Schrödinger perturbation theory. These weights quantify the effective contribution of the basis states (m) to the perturbed state of interest (n). The criterion for keeping state m in the basis is that the weight W is larger than a chosen number. While this method normally works very well, in the present case the above criterion would require to take into account many leaky and Fabry-Perot modes which in reality do not help much to reduce the error. We have therefore modified this criterion by simply taking

into account only the WG modes of the basis system, i.e. all the RSs with $|k| < lR/n_{b_0}$, in accordance with the condition for total internal reflection.

Figure S10 demonstrates results for one, two, three, and all four pairs of WG modes positioned symmetrically with respect to the imaginary k-axis ($N = 2$, 4, 6, and 8, respectively). It shows a vast improvement compared to single-mode approximations (diagonal, $N = 1$). Interestingly, adding to the basis only the conjugated mode on the other side of the spectrum ($N = 2$) already improves the result significantly. Taking all four WG modes and their counterparts ($N = 8$) provides nearly a full visual agreement with the exact solution, seen in Fig. S10(a) and in the inset to Fig. S8. Adding to this basis more modes increases the error, unless a really large number of basis states is included.

C. Comparison with other approximations

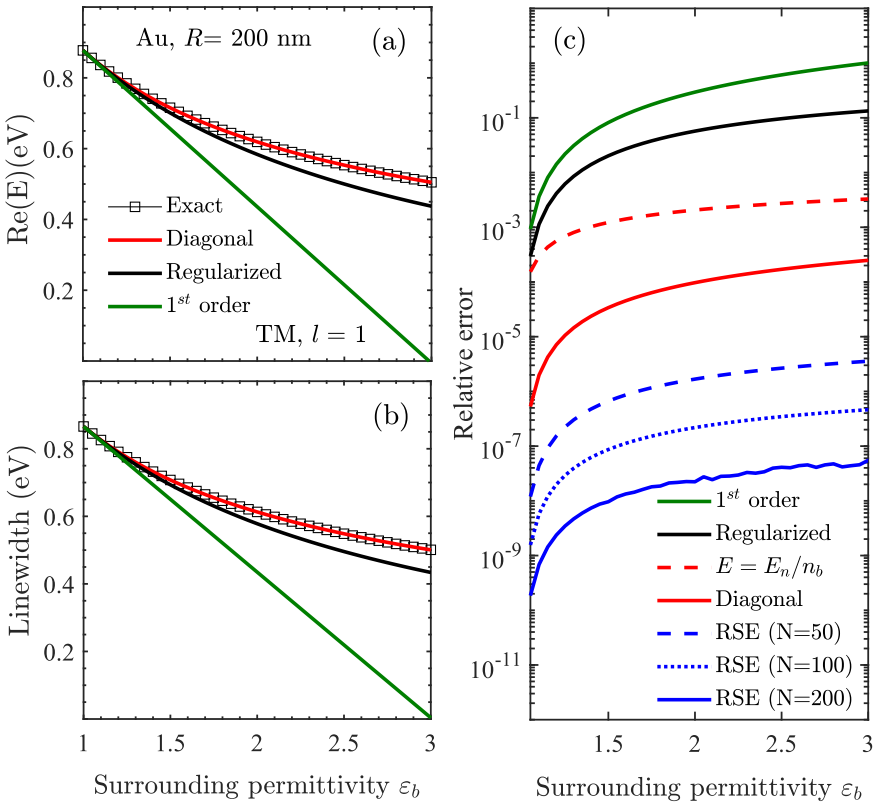

FIG. S11. As Fig. 2 of the main text but with regularized (black) and simple diagonal (dashed cyan) approximations added.

In Figs. S11, S12, and S13 we reproduce, respectively, Figs. 2, 3, and 4 of the main text, with two more approximations added for comparison: The regularized solution Eq. (S67)

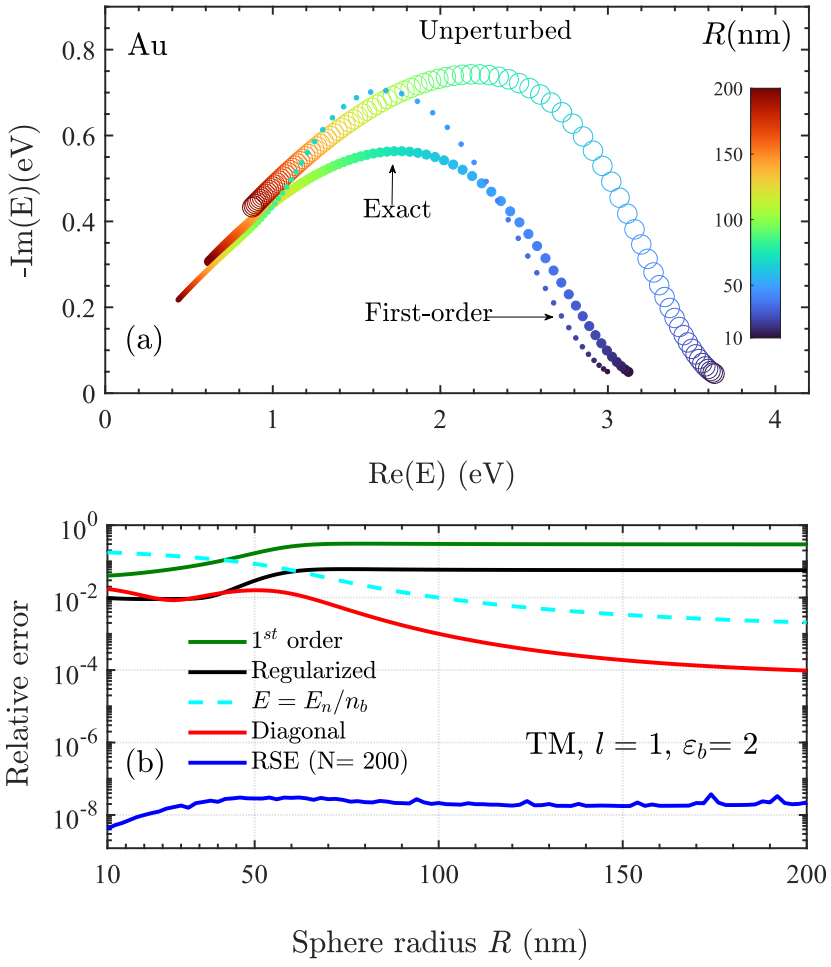

FIG. S12. As Fig. 3 of the main text but with regularized (black) and simple diagonal (dashed cyan) approximations added in (b).

and a simple diagonal approximation,

$$k_\nu \approx k_n n_{b_0}/n_b\,, \tag{S110}$$

obtained from the full diagonal solution Eq. (S31) by neglecting any matrix elements of the effective perturbation.

The full diagonal approximation shows at least an order of magnitude reduction of the error compared to Eq. (S110), even for small radii, as it is clear from Fig. S12. At the same time, the first-order approximation fails quickly as ε_b deviates from 1, as demonstrated by Fig. S11. Interestingly, the single-mode regularized version gives a reasonable agreement with the exact solution for the whole range of permittivities and radii considered. Looking at the relative errors shown in Fig. S13(d) for the silver bow-tie antenna, we see that all the approximations work effectively the same way as for a silver sphere of radius $R = 40\,\text{nm}$ in

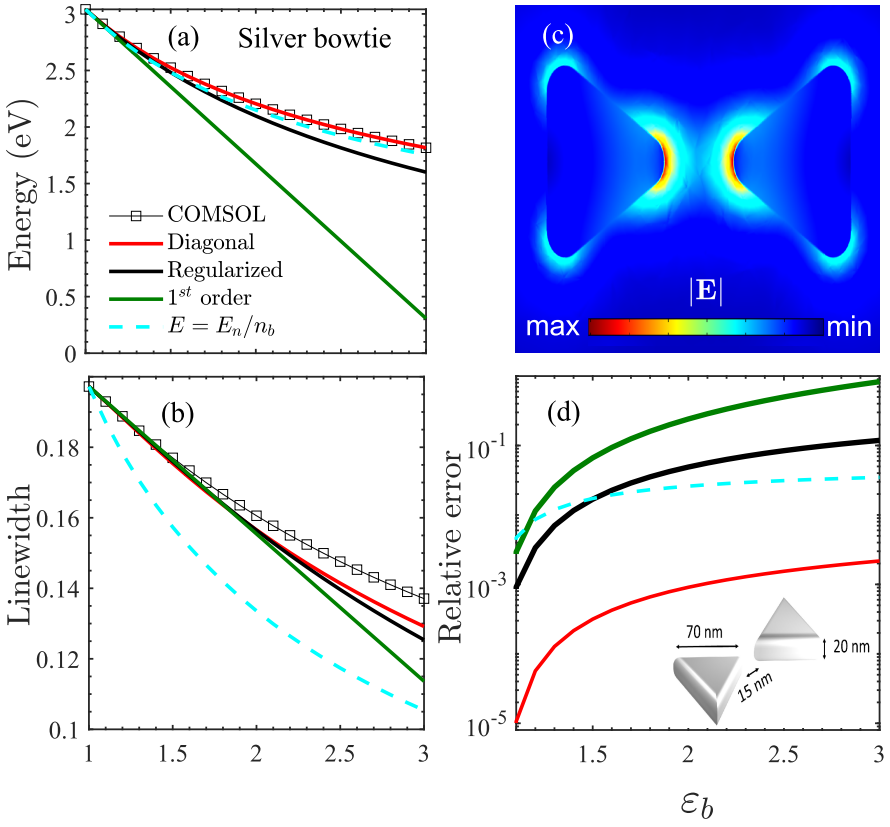

FIG. S13. As Fig. 4 of the main text but with regularized (black) and simple diagonal (dashed cyan) approximations added.

Fig. S14, demonstrating that the quality of the approximations is independent of the shape of an optical system (but depends on the effective size of the resonator, as demonstrated by Fig. S12).

D. Normalization and pertubation matrix elements for RSs calculated numerically

To apply the single-mode approximation [given by Eq. (S31) or Eq. (11) of the main text] to a numerically calculated basis RS, we need to evaluate the matrix element of the perturbation, given by Eq. (S20) for $n = m$, which is proportional to an integral over the system volume of the square of the electric and/or magnetics fields. The latter have to be correctly normalized, which also involves calculating volume and surface integrals of the field squared, according to Eq. (S44). Alternatively, one could employ the PML normalization introduced in [S10]. Numerical evaluation of these integrals, however, may carry in significant inaccuracies due to the finite grid and field uncertainty increasing at the edges of the system. We therefore deploy instead the high accuracy of Eq. (S31) to introduce a practical method of evaluating these integrals by using only the numerical values of the RS wave number

calculated for the unperturbed system and for the same system in a very slightly perturbed medium. To illustrate the idea, let us consider for simplicity a non-magnetic, non-chiral but generally dispersive system which can be split into J pieces, each piece described by a homogeneous isotropic permittivity $\varepsilon_j(k)$. Then Eq. (S31) can be written as

$$1-\chi_\nu=\sum_{j=1}^{J} I_j\left[(\chi_\nu-1)\Delta\varepsilon_j(\infty)+\Delta\varepsilon_j(k_n)\right], \tag{S111}$$

where

$$I_j=\int_{\mathcal{V}_j}\mathbf{E}_n^2(\mathbf{r})d\mathbf{r} \tag{S112}$$

is the integral of the square of the electric field of the unperturbed RS (with the wave number k_n) over the volume $\mathcal{V}_j$ of the j-th part of the system,

$$\chi_\nu=\frac{k_\nu}{\Gamma k_n}, \tag{S113}$$

and

$$\Delta\varepsilon_j(k)=\alpha^2\varepsilon_j(\Gamma k)-\varepsilon_j(k), \tag{S114}$$

in accordance with Eq. (6) of the main text. The unknown J integrals I_j can then be determined from solving J linear simultaneous equations, for which one can provide J different values of the perturbed wave number k_ν and one unperturbed wave number k_n, in this way performing $J+1$ calculations for different values of the surrounding permittivity ε_b. Furthermore, for small deviations of ε_b from ε_{b0} (e.g. below 0.005% as used in the examples below), Eq. (S111) simplifies to

$$1-\chi_\nu=(\alpha-1)\sum_{j=1}^{J} I_j\left[k\varepsilon_j(k)\right]'_{k=k_n}. \tag{S115}$$

After all I_j are determined, stronger perturbations of the environment are accurately calculated via Eq. (S111).

The above method enables us to overcome the difficulty of normalizing RSs for complicated system's shapes since it relies only on determining of $J+1$ eigen wave numbers, which can obtained numerically or even experimentally. We note that calculating the wave numbers numerically for small changes of the environment does not require repetitive optimization of the simulation model, such as changing the initial guess or the PML thickness. Its presents an accurate evaluation of the matrix element of the perturbation as demonstrated by examples in Sec. S.V E. We use this matrix element for the single-mode approximations, including both the diagonal and first-order approximations.

E. Other COMSOL calculations

In addition to the data on silver bow-tie antenna presented in the main text, here we provide more examples of non-spherical systems in which RSs are calculated numerically using

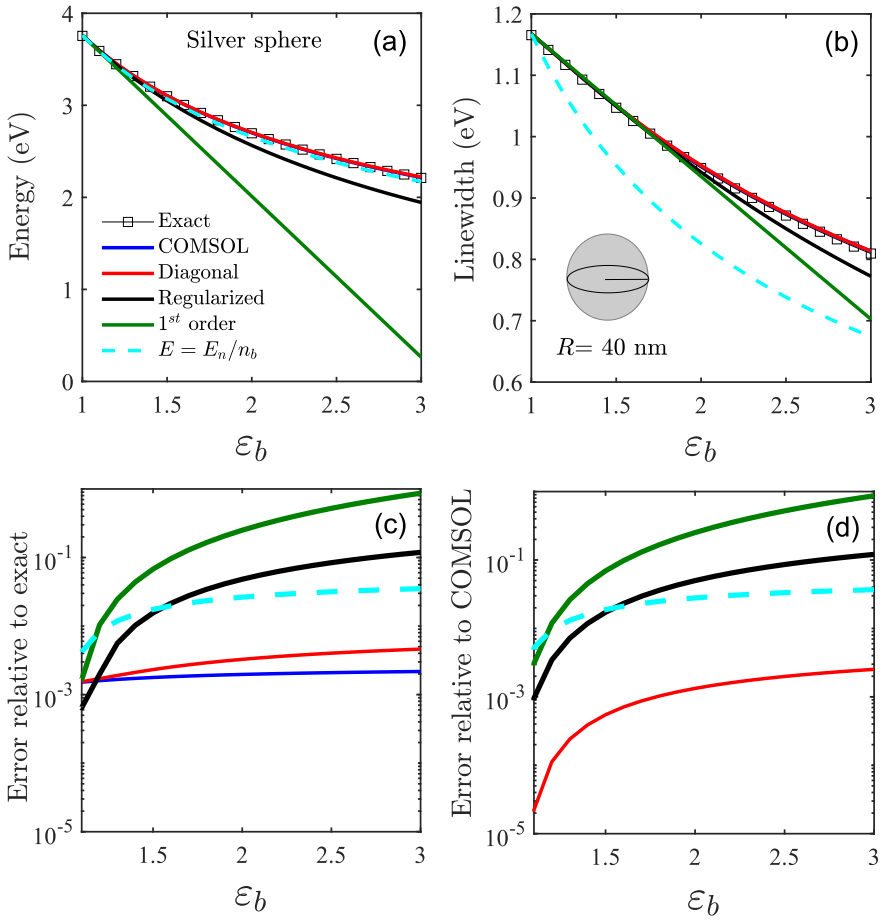

FIG. S14. Energy (a) and linewidth (b) calculated by using the exact analytic secular equation (squares), COMSOL (blue line), diagonal RSE (red line), regularized (black line), first-order (green line) and the simple approximation $E = E_n/n_b$ (dashed cyan) for the $l = 1$ TM fundamental SP mode of a silver sphere of $R = 40\,\text{nm}$ for varying permittivity of the surrounding medium ε_b, with the error of each method shown relative (c) to the exact and (d) to the COMSOL data. (c) also includes the COMSOL error relative to the exact solution (blue line).

the finite-element method implemented in COMSOL. This is done by using an open-source software Modal Analysis of Nanoresonators (MAN-7.1), which is an extension to COMSOL multiphysics built-in solver for computing the RSs in dispersive optical resonators [S11, S19]. These numerical RSs are used as basis states for applying the diagonal approximations developed in this work and also as an accurate solution (replacing the exact one which is not available in non-spherical systems) taken for comparison with the approximations.

To apply the single-mode approximations to a numerically calculated basis RS, we use the method of evaluation of the diagonal matrix element of the perturbation described in Sec. S.V D. We start from a verification of this approach in an exactly solvable system, which is a plasmonic nanosphere in vacuum. Here, we compare the accuracy of the modes,

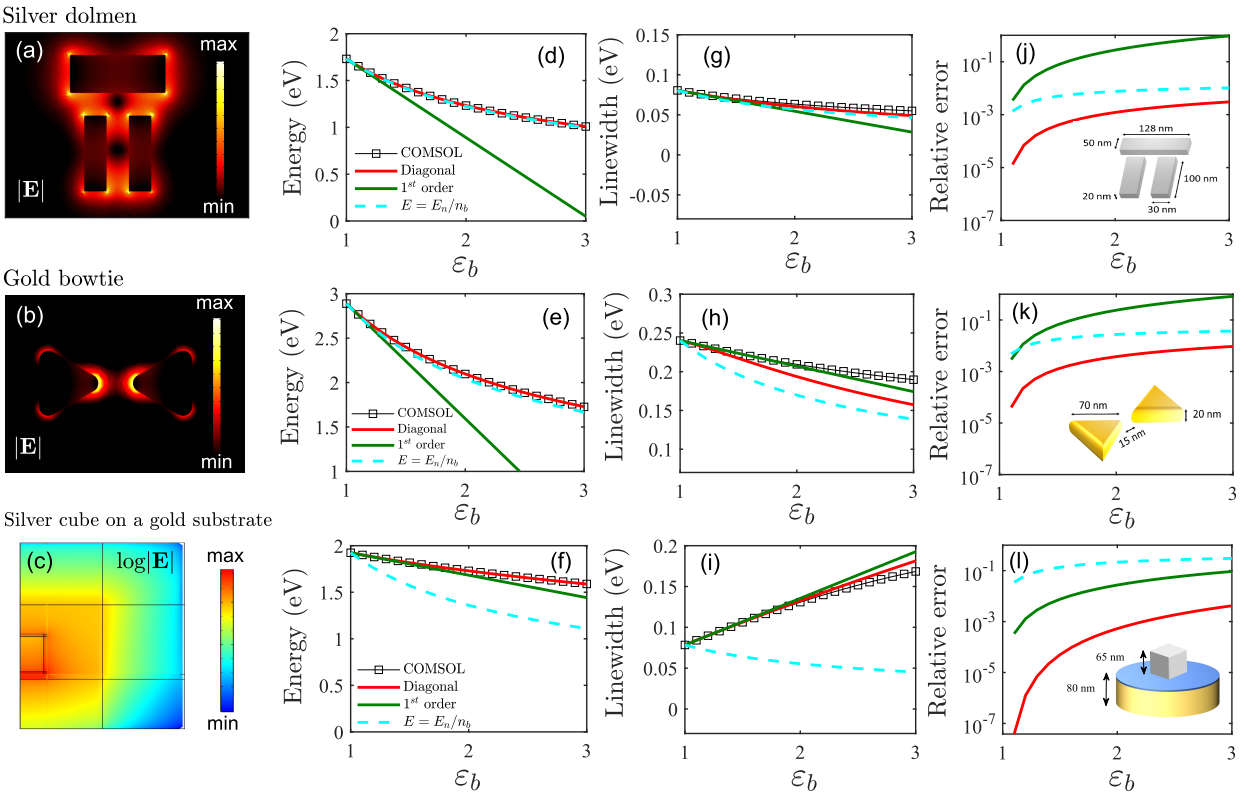

FIG. S15. Electric field of the fundamental SP mode of (a) silver dolmen, (b) gold bow-tie resonator and (c) silver cube on a gold substrate in vacuum. (d,e,f) Energy and (g,h,i) linewidth of the SP mode of, respectively, silver dolmen, gold bow-tie, and cube resonators calculated using COMSOL (thin lines with squares), the diagonal (red line), first order (green line) and the simple approximation $E = E_n/n_b$ (dashed cyan line). (j,k,l) Error of each approximation relative to COMSOL, with insets showing the structure of the resonator in each case.

calculated by COMSOL and via diagonal approximations, to the exact solution of the secular equation for TM polarization and $l = 1$, for a silver sphere of radius $R = 40\,\text{nm}$. The Drude parameters of silver are taken the same as in the main text. Figures S14(a) and (b) show both the analytical and COMSOL calculations of the energy and linewidth of the localized SP mode of the silver sphere as functions of the permittivity of the surrounding medium ε_b, along with all the diagonal approximations based on the numerical basis RS at $\varepsilon_b = \varepsilon_{b0} = 1$. We also show in Figs. S14(c) and (d) the errors of all the approximations relative, respectively, to the exact solution and to the COMSOL data.

We then apply the same method to calculation of perturbed RS wave numbers for different non-spherical systems and different materials, such as silver dolmen, silver and gold bow-tie antennas, and a silver cube resonator on a gold substrate, see Fig. S13, Fig. S15, and Fig. 4 of the main text. While the main message of our paper is about treating homogeneous changes in the unbounded space surrounding the system accurately, we show that the diagonal

approximation works well also for a resonator placed on a substrate. This was performed by including the system and its substrate in the effective system and mapping the external perturbation into the whole configuration, consisting of the system and the substrate.

In the considered examples, the following parameters were used. The width of the top rod in the dolmen structure is 128 nm and the length is 50 nm. The vertical rods are 100 nm long, 30 nm wide, and 20 nm thick. The gold bow-tie antenna has a side length of 70 nm and a thickness of 20 nm, the same parameters as of the silver bow-tie resonator in the main text. The cube resonator has a side of 65 nm, with corners rounded to arcs with a radius of 4 nm and the substrate has 80 nm thickness separated by 8 nm wide polymer. The Drude parameters of silver are taken the same as in the main text, while gold parameters generated by the program in [S3] are $\varepsilon_\infty = 1$, $\hbar c\sigma = 801.6\,\mathrm{eV}$, and $\hbar c\gamma = 0.085\,\mathrm{eV}$. The polymer beneath the cube has the permittivity of $\varepsilon = 2.25$. All single-mode approximations show similar level of accuracy across the systems treated. The deviation of the simple approximation Eq. (S110) for the cube on a substrate, both for the energy in Fig. S15(f) and the linewidth in Fig. S15(i), is attributed to a significant increase in the volume of the system due to the presence of the substrate.

[S1] E. A. Muljarov and T. Weiss, Resonant-state expansion for open optical systems: generalization to magnetic, chiral, and bi-anisotropic materials, Opt. Lett. **43**, 1978 (2018).

[S2] E. A. Muljarov and W. Langbein, Resonant-state expansion of dispersive open optical systems: Creating gold from sand, Phys. Rev. B **93**, 075417 (2016).

[S3] H. S. Sehmi, W. Langbein, and E. A. Muljarov, Optimizing the drude-lorentz model for material permittivity: Method, program, and examples for gold, silver, and copper, Phys. Rev. B **95**, 115444 (2017).

[S4] H. S. Sehmi, W. Langbein, and E. A. Muljarov, Applying the resonant-state expansion to realistic materials with frequency dispersion, Phys. Rev. B **101**, 045304 (2020).

[S5] S. Both and T. Weiss, First-order perturbation theory for changes in the surrounding of open optical resonators, Opt. Lett. **44**, 5917 (2019).

[S6] A. Baz', Y. Zel'dovich, and A. Perelomov, *Scattering, Reactions and Decay in Nonrelativistic Quantum Mechanics* (U. S. Department of Commerce, Washington, D. C., 1969).

[S7] R. C. Mcphedran and B. Stout, 'killing mie softly': Analytic integrals for complex resonant states, Quarterly Journal of Mechanics and Applied Mathematics **73**, 119 (2020).

[S8] P. T. Leung, S. Y. Liu, S. S. Tong, and K. Young, Time-independent perturbation theory for quasinormal modes in leaky optical cavities, Phys. Rev. A **49**, 3068 (1994).

[S9] J. P. Hugonin and P. Lalanne, Perfectly matched layers as nonlinear coordinate transforms: a generalized formalization, J. Opt. Soc. Am. A **22**, 1844 (2005).

[S10] C. Sauvan, J. P. Hugonin, I. S. Maksymov, and P. Lalanne, Theory of the spontaneous optical

emission of nanosize photonic and plasmon resonators, Phys. Rev. Lett. **110**, 237401 (2013).

[S11] W. Yan, R. Faggiani, and P. Lalanne, Rigorous modal analysis of plasmonic nanoresonators, Phys. Rev. B **97**, 205422 (2018).

[S12] E. A. Muljarov, W. Langbein, and R. Zimmermann, Brillouin-wigner perturbation theory in open electromagnetic systems, Europhys Lett. **92**, 50010 (2010).

[S13] E. A. Muljarov, Full electromagnetic green's dyadic of spherically symmetric open optical systems and elimination of static modes from the resonant-state expansion, Phys. Rev. A **101**, 053854 (2020).

[S14] M. B. Doost, W. Langbein, and E. A. Muljarov, Resonant-state expansion applied to three-dimensional open optical systems, Phys. Rev. A **90**, 013834 (2014).

[S15] E. A. Muljarov and W. Langbein, Exact mode volume and purcell factor of open optical systems, Phys. Rev. B **94**, 235438 (2016).

[S16] P. B. Johnson and R. W. Christy, Optical constants of the noble metals, Phys. Rev. B **6**, 4370 (1972).

[S17] M. D. Baaske, M. R. Foreman, and F. Vollmer, Single-molecule nucleic acid interactions monitored on a label-free microcavity biosensor platform, Nature Nanotechnology **9**, 933 (2014).

[S18] F. Vollmer and D. Yu, eds., *Optical Whispering Gallery Modes for Biosensing* (Springer International Publishing, 2020).

[S19] Modal Analysis of Nanoresonators (MAN-7.1) (https://www.lp2n.institutoptique.fr/light-complex-nanostructures).